

TOPICAL REVIEW

Axial structure of the nucleon

Véronique Bernard[†], Latifa Elouadrhiri[‡], Ulf-G Meißner[§][†] Université Louis Pasteur de Strasbourg, Groupe de Physique Théorique, F-67084 Strasbourg Cedex 2, France[‡] Thomas Jefferson National Accelerator Facility, Newport News, VA 23606, USA[§] Forschungszentrum Jülich, Institut für Kernphysik (Theorie), D-52425 Jülich, Germany

E-mail: bernard@lpt6.u-strasbg.fr, latifa@jlab.org, u.meissner@fz-juelich.de

Abstract. We review the current status of experimental and theoretical understanding of the axial nucleon structure at low and moderate energies. Topics considered include (quasi)elastic (anti)neutrino–nucleon scattering, charged pion electroproduction off nucleons and ordinary as well as radiative muon capture on the proton.

PACS numbers: 11.40.-q, 25.30.Rw, 23.40.-s, 25.30.Pt, 12.39.Fe

Submitted to: *J. Phys. G: Nucl. Part. Phys.*

1. Introduction

The structure of the nucleon in the non-perturbative regime of QCD can be characterized by a collection of scales, related to the probe which is used to study this basic building block of atomic nuclei. The typical nucleon size as deduced from electron scattering experiments is about 0.85 fm, whereas model–dependent analyses of proton–antiproton annihilation lead to a baryon charge radius of about 0.5 fm. An intermediate scale is set by the weak charged currents, which allows to measure the axial charge radius, $r_A \simeq 0.65$ fm, and related moments. For a more detailed discussion of these various scales and how they can be understood in a simple model, see reference [1]. Here, we will be concerned with nucleon matrix elements of the axial current, giving a status report on our current knowledge about the pertinent coupling constants and form factors, with particular emphasis on the theoretical methods which are used to extract this information from experiment. Our basic object is the QCD axial current, expressed in terms of the light quark fields

$$A_\mu^a = \bar{q} \gamma_\mu \gamma_5 T^a q , \quad (1)$$

where for the two and three flavor case, the pertinent quark fields, generators and flavor indices are given by

	SU(2)	SU(3)	
q	$\begin{pmatrix} u \\ d \end{pmatrix}$	$\begin{pmatrix} u \\ d \\ s \end{pmatrix}$	(2)
T^a	$\tau^a / 2$	$\lambda^a / 2$	
a	1, 2, 3	1, ..., 8	

with τ^a the conventional Pauli isospin matrices and the λ^a are Gell-Mann's SU(3) matrices. Note that we do not consider the singlet components corresponding to $a = 0$ in what follows. To be specific, consider the matrix–element of the SU(2) isovector axial quark current between nucleon states,

$$\langle N(p') | A_\mu^a | N(p) \rangle = \bar{u}(p') \left[\gamma_\mu G_A(t) + \frac{(p' - p)_\mu}{2m} G_P(t) \right] \gamma_5 \frac{\tau^a}{2} u(p), \quad (3)$$

with $t = (p' - p)^2$ the invariant momentum transfer squared and $m = (m_p + m_n)/2$ the nucleon mass. Note that in this review, we mostly consider the isospin symmetric case and only differentiate between the proton (m_p) and the neutron (m_n) masses in kinematical factors. The form of equation (3) follows from Lorentz invariance, isospin conservation and the discrete symmetries C, P and T and the absence of second class currents [2], which is consistent with experimental information, see e.g. reference [3]. $G_A(t)$ is called the nucleon axial form factor and $G_P(t)$ the induced pseudoscalar form factor. Consider first the axial form factor, which probes the spin–isospin distribution of the nucleon (since in a non–relativistic language, this is nothing but the matrix–element of the Gamov–Teller operator $\sigma \tau$). The axial form factor admits the following expansion for small momentum transfer

$$G_A(t) = g_A \left(1 + \frac{1}{6} \langle r_A^2 \rangle t + O(t^2) \right), \quad (4)$$

with g_A the axial–vector coupling constant, $g_A = 1.2673 \pm 0.0035$ [4], and $\langle r_A^2 \rangle^{1/2}$ the nucleon axial radius. The experimental determinations and theoretical understanding of this fundamental low–energy observable will constitute a main part of this review. The axial–vector coupling constant is measured in (polarized) neutron beta–decay, for recent references see e.g. [5, 6]. Here, we will not discuss the determinations of g_A and of the related CKM matrix–element V_{ud} , for a review see [7]. For low and moderate momentum transfer, say $|t| \leq 1 \text{ GeV}^2$, the axial form factor can be represented by a dipole fit

$$G_A(t) = \frac{g_A}{(1 - t/M_A^2)^2}, \quad (5)$$

in terms of one adjustable parameter, M_A , the so–called axial mass (or sometimes dipole mass). Therefore, one can express the axial radius in terms of the dipole mass

$$\langle r_A^2 \rangle = \frac{6}{g_A} \left. \frac{dG_A(t)}{dt} \right|_{t=0} = \frac{12}{M_A^2}. \quad (6)$$

The induced pseudoscalar form factor is believed to be understood in terms of pion pole dominance and we will discuss the theoretical status concerning the corrections to this leading order term. Most measurement of this form factor stem from ordinary muon capture on the proton, $\mu^- + p \rightarrow \nu_\mu + n$. More precisely, in that reaction one measures the induced pseudoscalar coupling constant g_P ,

$$g_P = \frac{M_\mu}{2m} G_P(t = -0.88M_\mu^2) , \quad (7)$$

with M_μ the muon mass. This coupling constant is nothing but the value of the induced pseudoscalar form factor $G_P(t)$ at the four-momentum transfer for muon capture by the proton at rest,

$$t = -M_\mu^2 \left[1 - \frac{(M_\mu + m_p)^2 - m_n^2}{M_\mu(M_\mu + m_p)} \right] = -0.88 M_\mu^2 . \quad (8)$$

In what follows, we will review these determinations and also discuss radiative muon capture as well as pion electroproduction which allow to investigate the momentum dependence of $G_P(t)$.

The material is organized in the following way. In section 2, we collect the available data on the axial form factor $G_A(t)$, the induced pseudoscalar coupling constant g_P and the corresponding form factor $G_P(t)$. Section 3 is devoted to the theoretical methods which allow to determine the axial form factor and the axial radius of the nucleon as well as the pion charge radius from (anti)neutrino scattering and pion electroproduction data. The QCD analysis of the induced pseudoscalar form factor and the methods to extract it from ordinary and radiative muon capture are discussed in section 4. Section 5 is devoted to a discussion of certain axial matrix elements in the baryon octet pertinent to the quark mass analysis. A short summary and outlook are given in section 6. Before proceeding, we point out that in this review *no* model calculations of the matrix elements are reviewed, as illustrative as they might be. Our emphasis is on applying a model-independent approach tightly constrained by the symmetries of the Standard Model to determine the axial structure of the nucleon in the non-perturbative regime.

2. Data overview

In this section, we will give a brief review of published data on the axial and induced pseudoscalar form factors. The methods which lead to these results will be presented and critically discussed in the following sections. At this point, we only wish to point out that systematical errors for certain processes have certainly been underestimated, but here we simply collect the data as they are available.

2.1. Data on the axial form factor

There are two methods to determine the axial form factor of the nucleon, namely (anti)neutrino scattering off protons or nuclei and charged pion electroproduction. We consider first the experimental data coming from measurements of (quasi)elastic

(anti)neutrino scattering off protons [8, 9, 10], off deuterons [11]-[16] and other nuclei (Al, Fe) [17, 18] or composite targets like freon [19]-[22] and propane [22, 23]. In the left panel of figure 1 we show the available values for the axial mass M_A obtained from neutrino scattering experiments. As pointed out in [24], references [17, 19, 20, 23] reported

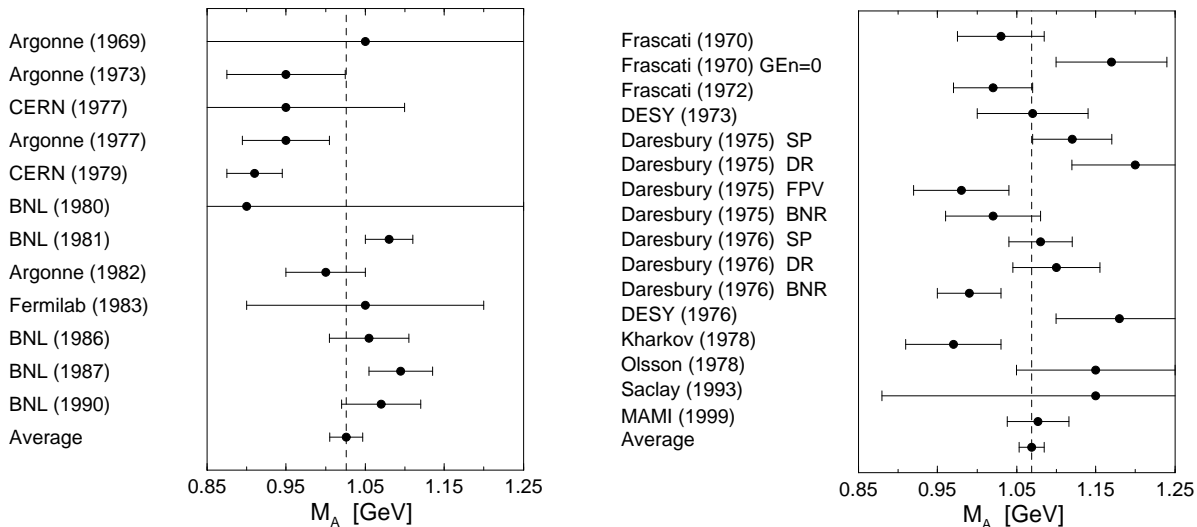


Figure 1. Axial mass M_A extractions. Left panel: From (quasi)elastic neutrino and antineutrino scattering experiments. The weighted average is $M_A = (1.026 \pm 0.021)$ GeV. Right panel: From charged pion electroproduction experiments. The weighted average is $M_A = (1.069 \pm 0.016)$ GeV. Note that value for the MAMI experiment contains both the statistical and systematical uncertainty; for other values the systematical errors were not explicitly given. The labels SP, DR, FPV and BNR refer to different methods evaluating the corrections beyond the soft pion limit as explained in the text.

severe uncertainties in either knowledge of the incident neutrino flux or reliability of the theoretical input needed to subtract the background from genuine elastic events (both of which gradually improved in subsequent experiments). The values derived in these papers fall well outside the most probable range of values known today and exhibit very large statistical and systematical errors. Following the data selection criteria of the Particle Data Group [4], they were excluded from this compilation. In all cases, the axial form factor data were parameterized in terms of a dipole, the resulting world average is

$$M_A = (1.026 \pm 0.021) \text{ GeV} \quad (\text{neutrino scattering}) . \quad (9)$$

The other determinations of the axial form factor are based on the analysis of charged pion electroproduction off protons, see references [24][25]-[34], slightly above the pion production threshold (note that the MAMI measurement is presently extended [35] to lower momentum transfer and to check the cross section at the highest Q^2 point reported in [24]). Such type of analysis is more involved. It starts from the low-energy theorem of Nambu, Lurié and Shrauner [36, 37] for the electric dipole amplitude $E_{0+}^{(-)}$ at threshold,

valid for soft pions, i.e. pions with vanishing four-momentum. Model-dependent corrections (so-called hard pion corrections) were developed to connect the low-energy theorem to the data, that is to the real world with a finite pion mass, see references [38]-[45], labeled SP, FPV, DR and BNR, respectively. For a given model, the values of the axial mass were determined from the slopes of the angle-integrated differential electroproduction cross sections at threshold. The results of various measurements and theoretical approaches are shown in the right panel of figure 1. Note again that references [27, 38] were omitted from the fit for lack of reasonable compatibility with the other results. In figure 2 we have collected the various electroproduction data, in comparison

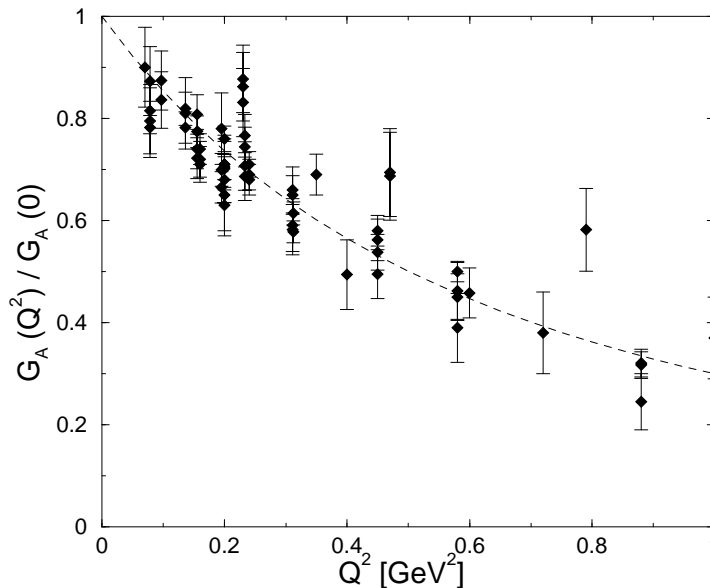


Figure 2. Experimental data for the normalized axial form factor extracted from pion electroproduction experiments in the threshold region. Note that for the experiments where various theoretical models were used in the analysis to extract G_A , all results are shown. For orientation, the dashed line shows a dipole fit with an axial mass $M_A = 1.1$ GeV.

to a dipole fit with $M_A = 1.1$ GeV. Again, at various values of the momentum transfer one sees two or three data points, these show the model-dependence due to the applied hard pions corrections. The resulting world average of the dipole masses collected in figure 1 is

$$M_A = (1.069 \pm 0.016) \text{ GeV} \quad (\text{electroproduction}) . \quad (10)$$

Although some of these results have large uncertainties, the weighted average for the axial mass determinations from neutrino scattering and pion electroproduction are quite precise. In particular, we notice an *axial mass discrepancy*, i.e. the so determined axial masses differ significantly,

$$\Delta M_A = (0.043 \pm 0.026) \text{ GeV} , \quad (11)$$

which translates into an axial radius difference of about 5%, i.e. the axial radius of the nucleon determined from neutrino scattering data appears bigger than the one from electroproduction, $\langle r_A^2 \rangle_{\nu\text{-scatt.}}^{1/2} = (0.666 \pm 0.014)$ fm versus $\langle r_A^2 \rangle_{\text{elprod.}}^{1/2} = (0.639 \pm 0.010)$ fm, the *axial radius discrepancy* to be discussed in section 3.

2.2. Data on the induced pseudoscalar form factor

Ordinary muon capture (OMC),

$$\mu^-(l) + p(r) \rightarrow \nu_\mu(l') + n(r') , \quad (12)$$

where we have indicated the four-momenta of the various particles, allows to measure the induced pseudoscalar coupling constant, g_P . Most experiments so far have used liquid hydrogen targets, which leads to atomic physics complications because the μp atom rapidly forms an $p\mu p$ orthomolecule. Consequently, one has to know the transition rate from the ortho to the para ground state. Furthermore, there can be mixing between $S = 1/2$ and $S = 3/2$ components of the ortho $p\mu p$ state [46]. To facilitate the discussion, the various atomic and molecular states are shown in figure 3 together with the pertinent transition rates (as determined experimentally). The world data on

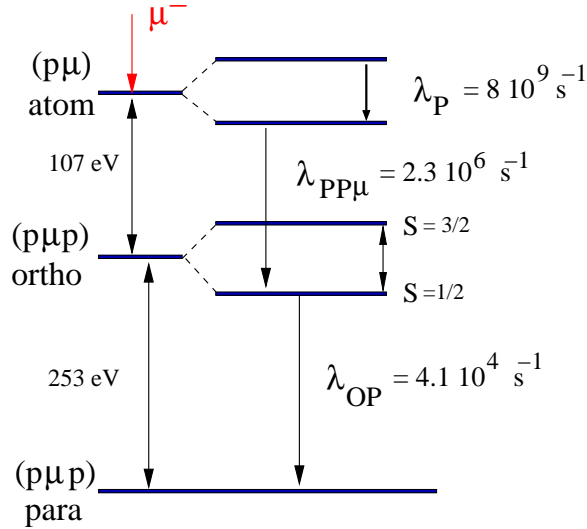


Figure 3. Level scheme for OMC in liquid hydrogen. In the atomic $(p\mu)$ state, one has a triplet/singlet state where the sum of the proton and the muon spins is $1/0$ (upper two levels). In the ortho $(p\mu p)$ state, the two proton spins sum up to one, splitting into two levels with $S = 3/2$ and $S = 1/2$ as indicated. Weinberg’s mixing suggestion [46] applies to these two levels.

electronics experiments for muon capture in hydrogen [47]-[52] are collected in figure 4, these values have been rescaled to the present day values of the axial-vector coupling constant, the Fermi constant and the Cabbibo angle. The weighted world average is

$$g_P = 8.79 \pm 1.92 , \quad (13)$$

which is in good agreement with theoretical expectations as discussed below. At this

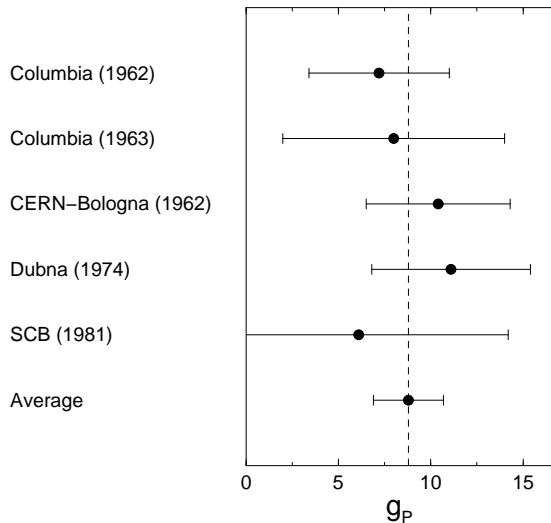


Figure 4. Determination of the pseudoscalar coupling constant g_P from (electronics) experiments. The numbers have been rescaled to the present value of $g_A = 1.267$. For the measurements on liquid hydrogen, the rate $\lambda_{\text{OP}} = (4.1 \pm 1.4) \cdot 10^4 \text{ s}^{-1}$ is assumed. The weighted average is $g_P = 8.79 \pm 1.92$.

point it is worth to emphasize that the experimental value for the ortho–para transition rate $\lambda_{\text{OP}} = (4.1 \pm 1.4) \cdot 10^4 \text{ s}^{-1}$ [52] is used to arrive at the world average. This value disagrees, however, with the theoretical expectation of reference [53], $\lambda_{\text{OP}}^{\text{thy}} = (7.1 \pm 1.2) \cdot 10^4 \text{ s}^{-1}$. We also point out that the theoretical formula for the liquid capture rate à la [53] involves a time integration from zero to infinity while in the measurement only a finite time interval is considered, thus a direct comparison is dangerous. A similar observation has recently been made in reference [54]. Stated differently, the theory has to adopt to the experimental circumstances. We would like to stress here the importance of the new proposed experiment at PSI [55] which will be done with a hydrogen gas target and will thus be independent of possible molecular complications because one will directly measure the atomic singlet rate. This experiment attempts to measure g_P to one percent accuracy, which would be a significant improvement compared to the present situation. These topics will be taken up again in section 4. The induced pseudoscalar coupling constant has also been determined by muon capture on various nuclei, from light to heavy ones. A comprehensive review has been given in [56], here we only report results for some light nuclei in table 1. Note that these determinations are mostly in agreement with the theoretical expectations, but the spread in the results is larger than given in the table [56]. In heavier nuclei, there has been much discussion about a possible quenching of g_P (similar to the quenching of g_A), but the situation can not be considered settled. We do not pursue this topic here, but refer to the recent reference [57]. While the momentum transfer in OMC is fixed, *radiative muon capture* (RMC),

$$\mu^-(l) + p(r) \rightarrow \nu_\mu(l') + n(r') + \gamma(k) , \quad (14)$$

Table 1. Pseudoscalar coupling constant determined from OMC in light nuclei.

Nucleus	g_P	Reference
^3He (capture to triton)	8.6 ± 1.5	[58]
^{12}C (capture to ground state)	8.3 ± 2.5	[59]
^{16}O (capture to $^{16}\text{N}(0^-)$)	10.0 ± 1.2	[60] [61]

has a variable momentum transfer t and one can get up to $t = M_\mu^2$ at the maximum photon energy of about $k_0 \sim 100$ MeV, which is quite close to the pion pole. This amounts approximately to a four times larger sensitivity to g_P in RMC than OMC. However, this increased sensitivity is upset by the very small partial branching ratio in hydrogen ($\sim 10^{-8}$ for photons with $k_0 > 60$ MeV) and one thus has to deal with large backgrounds. Precisely for this reason only very recently a first measurement of RMC on the proton has been published [62, 63]. The resulting number for g_P , which was obtained using a relativistic tree model including the Δ -isobar [64] to fit the measured photon spectrum, came out significantly larger than expected from OMC,

$$g_P^{\text{RMC}} = 12.35 \pm 0.88 \pm 0.38 \simeq 1.4 g_P^{\text{OMC}} , \quad (15)$$

and thus also about 40% above all theoretical expectations (see section 4.1). It should be noted that in this model the momentum dependence in $G_P(t)$ is solely given in terms of the pion pole and the induced pseudoscalar coupling is obtained as a multiplicative factor from direct comparison to the photon spectrum and the partial RMC branching ratio (for photon energies larger than 60 MeV). We will critically examine this procedure in section 4.3.2. It was also argued in [62, 63] that the atomic and molecular physics related to the binding of the muon in singlet and triplet atomic μp and ortho and para $p\mu p$ molecular states is sufficiently well under control (which is under debate, see section 4.2). This result spurred a lot of theoretical activity, as discussed later, but here we only wish to point that it is a viable possibility that the discrepancy does not come from the strong interactions but rather is related to the distribution of the various spin states of the muonic atoms. It is therefore mandatory to sharpen the theoretical predictions for the strong as well as the non-strong physics entering the experimental analysis. In principle, $G_P(t)$ can also be measured in pion electroproduction, because it enters the longitudinal cross section (in parallel kinematics) together with many other effects (see the discussion in section 3.4.4). However, the leading dependence due to the pion pole (and its chiral corrections) is unique and can be tested. So far there has only been one experiment [65] that took up the challenge, with the results shown in figure 5. The observed momentum dependence agrees with theoretical expectations, but a more refined measurement is certainly called for. In fact, at the Mainz Microtron MAMI-B a dedicated experiment has been proposed to measure the induced pseudoscalar form factor by means of charged pion electroproduction at low momentum transfer [66]. At this point, it is important to stress that in the low-energy region, $G_P(t)$ is not truly independent from $G_A(t)$, as discussed in detail in section 4.1. We conclude that the

induced pseudoscalar form factor is the least well known of all six electroweak nucleon form factors.

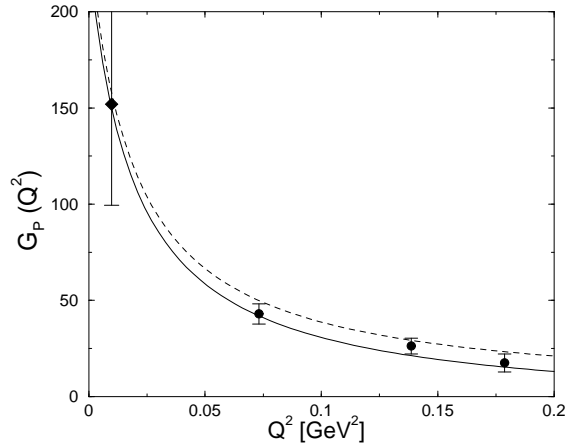


Figure 5. The “world data” for the induced pseudoscalar form factor $G_P(Q^2)$. The pion electroproduction data (filled circles) are from reference [65]. Also shown is the world average for ordinary muon capture at $Q^2 = 0.88M_\mu^2$ (diamond). For orientation, we also show the theoretical predictions discussed later. Dashed curve: Pion-pole (current algebra) prediction. Solid curve: Next-to-leading order chiral perturbation theory prediction.

3. Nucleon axial radius and form factor

3.1. Determination of the axial form factor I: Neutrino scattering formalism

Neutral and charged current (anti)neutrino scattering off protons or light nuclei can be used to extract the axial form factor. Since these topics are well documented in the literature [67, 68, 69], we only give some basic formulae (sometimes in a highly symbolic notation). The starting point is the effective Lagrangian of the electroweak Standard Model for elastic neutrino-hadron scattering, such as $\nu_\mu p \rightarrow \nu_\mu p$, or quasi-elastic scattering, such as $\nu_\mu n \rightarrow \mu^- p$ reactions (and similarly for anti-neutrinos),

$$\mathcal{L}^{\nu h} = -\frac{G_F}{\sqrt{2}} \bar{\ell} \gamma^\mu (1 + \gamma_5) \nu J_\mu^{\text{hadr}} + \text{h.c.} \quad (16)$$

with ℓ the neutrino/lepton in the final state. We are interested here in the hadronic current J_μ^{hadr} which can be written as

$$J_\mu^{\text{hadr}} = \alpha V_\mu^3 + \beta A_\mu^3 + \gamma V_\mu^0 + \delta A_\mu^0 + \dots, \quad (17)$$

where the up- and down-quark contributions are combined to form the isoscalar and isovector vector (V_μ^0, V_μ^3) and axial-vector currents (A_μ^0, A_μ^3). The ellipses represent heavy quark (s, c, b) terms. In the Standard Model, one has at tree level

$$\alpha = 1 - 2 \sin^2 \theta_W, \quad \beta = 1, \quad \gamma = -\frac{2}{3} \sin^2 \theta_W, \quad \delta = 0, \quad (18)$$

with θ_W the (weak) mixing angle. It describes the strength of the mixing of the electromagnetic current with the neutral weak current and thus only appears in the vector currents. Assuming now time reversal invariance, isospin invariance, the absence of second class currents, and neglecting the induced pseudoscalar form factor (in some analyses, this form factor is retained in its simplified pole form, $G_P(Q^2) \simeq 2mG_A(Q^2)/(Q^2 + M_\pi^2)$), the hadronic current matrix element between nucleon states is given by

$$\langle N(p') | J_\mu^{\text{hadr}} | N(p) \rangle = \bar{u}(p') \left[\gamma_\mu F_1(Q^2) + \frac{i\sigma_{\mu\nu}q^\nu}{2m} F_2(Q^2) + \gamma_\mu \gamma_5 G_A(Q^2) \right] u(p), \quad (19)$$

with $Q^2 = -(p' - p)^2 = -q_\mu q^\mu$ the squared momentum transfer. Because of vector current conservation, the Dirac and Pauli vector form factors appearing in equation (19) are the same as the ones measured in elastic electron–hadron scattering and can therefore be considered as known. What is usually assumed in the analysis of the neutrino scattering experiments is the dipole parameterization for the Sachs form factors, $G_E = F_1 + (Q^2/4m^2)F_2$ and $G_M = F_1 + F_2$. It has the form: $G_E^p = D$, $G_E^n = 0$, $G_M^{p/n} = \kappa_{p/n}D$, where $D = (1 + Q^2/M_V^2)^{-2}$, $\kappa_{p/n}$ is the proton/neutron magnetic moment and $M_V = 0.84 \text{ GeV}$. The axial form factor is then extracted by fitting the Q^2 -dependence of the (anti)neutrino-nucleon cross section,

$$\frac{d\sigma^{(\nu p, \bar{\nu} p)}}{dQ^2} = \frac{G_F m^2}{8\pi E_\nu} \left[A(Q^2) \mp B(Q^2) \frac{(s-u)}{m^2} + C(Q^2) \frac{(s-u)^2}{m^4} \right] \quad (20)$$

in which $G_A(Q^2)$ is contained in the bilinear forms $A(Q^2)$, $B(Q^2)$ and $C(Q^2)$ of the relevant form factors and is assumed to be the only unknown quantity

$$\begin{aligned} A &= \frac{4\tilde{Q}^2}{m^2} \left[(1 + \tau)G_A^2 - (1 - \tau)F_1^2 + \tau(1 - \tau)F_2^2 + 4\tau F_1 F_2 - \frac{M_\mu^2}{m^2} ((F_1 + F_2)^2 + G_A^2) \right], \\ B &= 4\tau G_A (F_1 + F_2), \\ C &= \frac{1}{4} [G_A^2 + F_1^2 + \tau F_2^2], \end{aligned} \quad (21)$$

where the plus sign is for neutrinos and the minus sign for antineutrinos, and

$$s - u = 4mE_\nu - \tilde{Q}^2, \quad \tau = \frac{Q^2}{4m^2} \quad (22)$$

with $\tilde{Q}^2 = Q^2 - M_\mu^2$ and M_μ the muon mass. Of course, for elastic scattering $(\bar{\nu}) p \rightarrow (\bar{\nu}) p$ the terms $\sim M_\mu$ should be dropped. Due to the smallness of the lepton mass, they are usually also dropped for the quasi-elastic reactions. Furthermore, E_ν is the neutrino energy which is usually determined from the neutrino flux spectrum. Using the the dipole parameterization equation (5) allows then to determine M_A from a fit to the measured (anti)neutrino cross section. Here, one assumes that heavy quark corrections to the axial current can be neglected, although they are not necessarily small [70, 71]. In particular, the so-called strange quark content of the nucleon has attracted much attention over the last decade. Since the Q^2 -dependence for such type of contribution is not known, one can simply modify the dipole ansatz to $G_A(Q^2) = G_{\text{dipole}}(Q^2)(1 + \eta)$, with η parameterizing the strange (heavy) quark contribution. We do not wish to further elaborate on this topic but rather refer to the references [10, 72].

3.2. Determination of the axial form factor II: Electroproduction formalism

Consider now pion electroproduction off nucleons,

$$\gamma^*(k^2) + N_1(p_1) \rightarrow \pi^a(q) + N_2(p_2) , \quad (23)$$

where γ^* denotes the virtual photon with virtuality $k^2 < 0$, $N_i(p_i)$ ($i = 1, 2$) the initial/final nucleon and $\pi^a(q)$ the pion with Cartesian isospin $a = (0, +, -)$ and four-momentum q_μ . We will also use the positive definite quantity $Q^2 = -k^2$. The pertinent Mandelstam variables are $s = (p_1 + k)^2$, $t = (p_1 - p_2)^2$ and $u = (p_1 - q)^2$, subject to the constraint $s + t + u = 2m^2 + M_\pi^2 + k^2$, with M_π the pion mass. In the Born (one-photon-exchange) approximation, the corresponding coincidence cross section can be factorized as [73]

$$\frac{d\sigma}{dE'_e d\Omega'_e d\Omega_\pi^*} = \Gamma_v \frac{d\sigma_v}{d\Omega_\pi^*} , \quad (24)$$

where Γ_v is the virtual photon flux, E'_e, Ω'_e the energy and the solid angle of the scattered electron, and $d\sigma_v/d\Omega_\pi^*$ is the virtual photon cross section in the centre-of-mass frame of the final πN system, as denoted by the star. It can be further decomposed into transverse, longitudinal and two interference parts,

$$\frac{d\sigma_v}{d\Omega_\pi^*} = \frac{d\sigma_T}{d\Omega_\pi^*} + \epsilon_L^* \frac{d\sigma_L}{d\Omega_\pi^*} + \sqrt{2\epsilon_L^*(1+\epsilon)} \frac{d\sigma_{LT}}{d\Omega_\pi^*} \cos\phi_\pi + \epsilon \frac{d\sigma_{TT}}{d\Omega_\pi^*} \cos 2\phi_\pi \quad (25)$$

with the transverse (ϵ) and longitudinal ($\epsilon_L^* = -k^2\epsilon/k_0^{*2}$) polarizations of the virtual photon fixed by the electron kinematics. In parallel kinematics ($\theta_\pi^* = \theta_\pi = 0^\circ$, with θ_π the polar angle in the scattering plane as seen in the laboratory system) the interference parts vanish. Therefore, at constant four-momentum transfer, the transverse and the longitudinal cross sections can be separated using the Rosenbluth method by varying ϵ ,

$$\frac{d\sigma_v}{d\Omega_\pi^*} = \frac{d\sigma_T}{d\Omega_\pi^*} - \epsilon \frac{k^2}{k_0^{*2}} \frac{d\sigma_L}{d\Omega_\pi^*} . \quad (26)$$

(Note that often the photon energy is denoted by ω , however, here this symbol is entirely reserved for the pion energy). At low energies, the connection to theory is most easily made by means of the multipole expansion. For doing that, one considers the transition current related to equation (23), which can be decomposed in terms of six invariant amplitudes (we follow the conventions and notations of reference [74], see also [75])

$$\epsilon \cdot T(p_2, s_2; q, a | p_1, s_1; k) = i \bar{u}_2 \gamma_5 \sum_{i=1}^6 \epsilon \cdot \mathcal{M}_i A_i(s, u) u_1 , \quad (27)$$

with s_i the spin index of nucleon i . The explicit forms of the operators \mathcal{M}_i can be found in [74] and the A_i are invariant functions that depend on two kinematical variables. Here, we have chosen the Mandelstam variables s and u . The amplitudes $A_i(s, u)$ have the isospin decomposition

$$A_i(s, u) = A_i^{(+)}(s, u) \delta_{a3} + A_i^{(-)}(s, u) \frac{1}{2} [\tau_a, \tau_3] + A_i^{(0)}(s, u) \tau_a . \quad (28)$$

In terms of the isospin components, the physical channels are given by

$$\begin{aligned}
 T_\mu(\gamma^*p \rightarrow \pi^+n) &= \sqrt{2} [T_\mu^{(0)} + T_\mu^{(-)}] , \\
 T_\mu(\gamma^*n \rightarrow \pi^-p) &= \sqrt{2} [T_\mu^{(0)} - T_\mu^{(-)}] , \\
 T_\mu(\gamma^*p \rightarrow \pi^0p) &= T_\mu^{(+)} + T_\mu^{(0)} , \\
 T_\mu(\gamma^*n \rightarrow \pi^0n) &= T_\mu^{(+)} - T_\mu^{(0)} ,
 \end{aligned} \tag{29}$$

where we have listed the neutral pion channels for completeness. Most of the following discussions will be focused on the first reaction. For the discussion of the low-energy theorems that link the axial form factor to the charged pion production amplitudes, we spell out the corresponding multipole decomposition of the transition current matrix element at threshold. In the γ^*N centre-of-mass system at threshold, i.e. for $q_\mu = (M_\pi, 0, 0, 0)$, one can express the current matrix element in terms of the two S-wave multipole amplitudes, called E_{0+} and L_{0+} ,

$$\boldsymbol{\epsilon} \cdot \mathbf{T} = 4\pi i(1 + \mu) \chi_f^\dagger \left\{ E_{0+}(\mu, \nu) + [L_{0+}(\mu, \nu) - E_{0+}(\mu, \nu)] \hat{k} \cdot \boldsymbol{\epsilon} \hat{k} \cdot \boldsymbol{\sigma} \right\} \chi_i , \tag{30}$$

with $\chi_{i,f}$ two-component Pauli-spinors for the nucleon. We have introduced the dimensionless quantities

$$\mu = \frac{M_\pi}{m} , \quad \nu = \frac{k^2}{m^2} . \tag{31}$$

The multipole E_{0+} characterizes the transverse and L_{0+} the longitudinal coupling of the virtual photon to the nucleon spin. For an explicit expression of these multipoles in terms of the A_i evaluated at threshold, $s_{\text{thr}} = m^2(1 + \mu)^2$ and $u_{\text{thr}} = m^2(1 - \mu - \mu^2 + \mu\nu)/(1 + \mu)$, we refer to [74]. As it will become clear in the following paragraphs, the two parameters defined in equation (31) will play the role of small expansion parameters in the QCD analysis of pion electroproduction.

3.3. Current algebra derivation

While the methods of current algebra (CA) should be considered outdated by now, we consider it nevertheless instructive to briefly review the CA argument which gives the link between charged pion electroproduction and the nucleon axial form factor. Using standard LSZ formalism, the transition matrix element can be written as

$$T_\nu^a = - \int d^4x e^{iq \cdot x} (\square + M_\pi^2) \langle N_2 | \mathcal{T} \pi^a(x) V_\nu(0) | N_1 \rangle , \tag{32}$$

with V_ν the electromagnetic current operator to which the nucleon couples, q_μ the pion four-momentum and \mathcal{T} is the conventional time-ordering operator. Inserting now the PCAC relation $\partial^\mu A_\mu^a(x) = M_\pi^2 F_\pi \pi^a(x)$ and performing a partial integration (note that while the meaning of the PCAC relation has been understood since long [76, 77], it does not offer a systematic way of calculating higher order corrections), one gets

$$T_\nu^a = \frac{M_\pi^2 - q^2}{M_\pi^2 F_\pi} \left(q^\mu P_{\mu\nu}^a + C_\nu^a \right) ,$$

$$\begin{aligned}
 F_{\mu\nu}^a &= i \int d^4x e^{iq \cdot x} \langle N_2 | \mathcal{T} A_\mu^a(x) V_\nu(0) | N_1 \rangle , \\
 C_\nu^a &= \int d^4x e^{iq \cdot x} \delta(x_0) \langle N_2 | [A_0^a(x), V_\nu(0)] | N_1 \rangle .
 \end{aligned} \tag{33}$$

Using now the CA relation $[A_0^a(x), V_\nu(0)] = i\epsilon^{a3b}\delta^3(\mathbf{x})A_\nu^b(0)$, one obtains in the soft pion limit $q^\mu \rightarrow 0$

$$T_\nu^a = i \frac{\epsilon^{a3b}}{F_\pi} \langle N_2(p_2) | A_\nu^b(0) | N_1(p_1) \rangle + \text{pole terms} . \tag{34}$$

The pertinent nucleon matrix element appearing here was already given in equation (3), i.e. it contains the axial form factor $G_A(k^2)$ in terms of the photon virtuality $k^2 < 0$, since in the soft-pion limit $q_\mu = 0$ the momentum transfer is $(p_2 - p_1)_\mu = k_\mu$. Because of the ϵ -tensor, the axial form factor can only appear in charged pion electroproduction. In the chiral limit, Nambu, Lurié and Shrauner [36, 37] have put this in the form of a low-energy theorem for the electric dipole amplitude $E_{0+}^{(-)}$,

$$E_{0+}^{(-)}(M_\pi = 0, k^2) = \sqrt{1 - \frac{k^2}{4m^2}} \frac{e}{8\pi F_\pi} \left\{ G_A(k^2) + \frac{g_A k^2}{4m^2 - 2k^2} G_M^v(k^2) \right\} , \tag{35}$$

with G_M^v the nucleon isovector magnetic form factor. The second term in this equation stems from the nucleon pole contribution in the chiral limit. Expanding this to $\mathcal{O}(k^2)$, one finds

$$E_{0+}^{(-)}(M_\pi = 0, k^2) = \frac{eg_A}{8\pi F_\pi} \left\{ 1 + \frac{k^2}{6} \langle r_A^2 \rangle + \frac{k^2}{4m} \left(\kappa_v + \frac{1}{2} \right) + \mathcal{O}(k^3) \right\} , \tag{36}$$

with κ_v the nucleon isovector anomalous magnetic moment. Of course, this equation is only correct for massless pions with zero three-momentum. Before the advent of chiral perturbation theory, there existed many prescriptions to get a handle on the corrections due to the pion mass, see references [38]-[45] For a textbook treatment of this issue, see e.g. reference [73]. This was already addressed in section 2 in connection with theoretical uncertainties of the axial form factor extracted from electroproduction based on various prescriptions to deal with the corrections beyond the soft-pion limit. These uncertainties can and have to be overcome using the modern methods discussed next. To end this section, we remark that in principle equation (34) should also include the induced pseudoscalar form factor. However, in soft-pion limit the $G_P(t)$ term is proportional to the photon momentum k_μ , and when contracted with the photon polarization vector, one obtains the structure $\boldsymbol{\epsilon} \cdot \mathbf{k} G_P(t)$. Therefore, the induced pseudoscalar form factor only contributes to the longitudinal cross section, more precisely to the longitudinal S-wave multipole L_{0+} (as discussed in section 3.4.4) but *not* to the transverse multipole E_{0+} which is entirely sensitive to the axial form factor (radius).

3.4. QCD analysis of charged pion electroproduction

3.4.1. Effective field theory of the Standard Model In this section, we briefly discuss the effective field theory of the Standard Model (SM), chiral perturbation theory, without giving any technical details. For that, we refer the reader to a number

of reviews [78, 79, 80, 81, 82]. At energies and momenta much below the scale set by the intermediate vector boson masses, the weak interactions are frozen and the $SU(3)_C \times SU(2)_L \times U(1)_Y$ Standard Model simplifies to $SU(3)_C \times U(1)$, i.e. QCD in the presence of QED. These two theories behave very differently at low energies. QED is characterized by a small coupling constant, $\alpha_{EM} = 1/137$, that means the photons and leptons almost decouple and very precise perturbative calculations can be performed. On the other hand, the QCD coupling constant becomes large at low energies, $\alpha_S = g_S^2/4\pi \simeq 1$ and the underlying fields (quarks and gluons) are confined within hadrons. Consequently, to study the strong interactions, one essentially has to consider QCD in the presence of external sources embodying the electroweak interactions. Apart from lattice gauge theory attempts, which are plagued by their own conceptual problems, no first principle calculations for this theory are possible. However, one can make use of the *symmetries* of QCD and their realizations to explore in a model-independent way the *chiral dynamics* of QCD. This is based on the observation that the six quark flavors fall into two distinct classes, the light (u,d,s) and the heavy (c,b,t) ones (light/heavy compared to the typical hadronic scale of 1 GeV). Therefore, to a good first approximation one can consider an ideal world with

$$m_u = m_d = m_s = 0, \quad m_c = m_b = m_t = \infty, \quad (37)$$

i.e. only the light flavors are active and the heavy ones decouple. This is called the chiral limit of QCD. The corresponding Lagrangian, \mathcal{L}_{QCD}^0 , contains only one parameter, g_S (or, by dimensional transmutation, Λ_{QCD}). \mathcal{L}_{QCD}^0 is highly symmetric because the gluon interactions with the quark triplet $q = (u, d, s)$ are flavor-blind. In particular, one can decompose the quark fields in left- and right-handed components. These can be independently transformed under $SU(3)_L$ and $SU(3)_R$ leaving \mathcal{L}_{QCD}^0 invariant. By Noether's theorem, this leads to eight conserved vector, $V_\mu^a = \bar{q}\gamma_\mu(\lambda^a/2)q$, and eight conserved axial-vector, $A_\mu^a = \bar{q}\gamma_\mu\gamma_5(\lambda^a/2)q$, currents. From these, one can construct conserved charges,

$$[Q_a^V, H_{QCD}^0] = [Q_a^A, H_{QCD}^0] \quad (a = 1, \dots, 8). \quad (38)$$

This is the so-called *chiral symmetry of the strong interactions*, which has indeed been observed long before the advent of QCD and led to current algebra and soft pion techniques (as used in the previous subsection). However, this symmetry is not necessarily shared by the ground state or the particle spectrum (hidden or spontaneously broken symmetry). So what is the fate of the chiral symmetry in QCD? For any vector-like gauge theory in the absence of θ -terms, one can show that the vacuum is invariant under vector transformations [83]. Concerning the axial transformations, nature selects the Nambu-Goldstone alternative, i.e. the ground state $|0\rangle$ is not symmetric and the left- and right-handed worlds communicate, as indicated by the non-vanishing quark condensate. Because the axial charges do not annihilate the vacuum, the spectrum must contain eight pseudoscalar Goldstone bosons, one for each broken generator. These particles have zero energy and three-momentum. As the energy/momentum transfer decreases, the interaction of the Goldstone bosons with themselves and matter becomes

weak, paving the way for a perturbative treatment in energies/momenta or a derivative expansion, despite the fact that the strong coupling constant is large. In the real world, the 8 lightest hadrons are indeed pseudoscalars (the three pions, four kaons and the eta). These particles are light but not exactly massless simply because the quark masses are not exactly zero but small. The QCD quark mass term therefore leads to explicit chiral symmetry breaking, which can be treated perturbatively. The important observation now is that the consequences of the broken chiral symmetry can be explored by means of an effective field theory, called *chiral perturbation theory* (CHPT). In essence, one maps the QCD Lagrangian on an effective Lagrangian formulated in terms of the asymptotically observed fields, the Goldstone bosons and matter fields (like nucleons),

$$\mathcal{L}_{\text{QCD}}[q, \bar{q}, g] \rightarrow \mathcal{L}_{\text{eff}}[U, \partial_\mu U, \dots, \mathcal{M}, \dots, N] , \quad (39)$$

where U collects the Goldstone bosons, the quark mass matrix \mathcal{M} parameterizes the explicit chiral symmetry breaking and matter fields N can also be included. For a deeper discussion of the foundations of CHPT, we refer to the seminal papers by Weinberg [84], Gasser and Leutwyler [85] and Leutwyler [86]. Observables are now expanded in powers of momenta (energies), generically called q , and quark masses, at a fixed ratio \mathcal{M}/q^2 . Stated differently, one has an underlying power counting [84] which allows one to organize any matrix–element M in terms of tree and loop diagrams for a given chiral dimension, symbolically

$$M = q^\nu f \left(\frac{q}{\mu}, g_i \right) , \quad (40)$$

where q is a small momentum or meson mass, f a function of order one, μ a regularization scale and g_i a collection of coupling constants. Because of chiral symmetry, the counting index (chiral dimension) ν is bounded from below. One can show that n –loop graphs are suppressed by powers of q^{2n} , thus the leading contribution to any given process stems from tree graphs with the lowest order insertions (which is equivalent to current algebra). To a given order, the corresponding effective Lagrangian must contain all terms compatible with chiral, gauge and discrete symmetries. Beyond leading order, such local interactions are accompanied by unknown coupling constants (the g_i in equation (40)), also called low–energy constants (LECs). While these can in principle be calculated from QCD, $g_i = g_i(\Lambda_{\text{QCD}}, m_c, m_b, m_t)$, in practice they must be determined by a fit to some data or estimated using some model. Let us illustrate this for the pion–nucleon system chirally coupled to external sources like e.g. electroweak gauge bosons. A complete one–loop calculation is based on the effective Lagrangian

$$\mathcal{L}_{\text{eff}} = \mathcal{L}_{\pi N}^{(1)} + \mathcal{L}_{\pi N}^{(2)} + \mathcal{L}_{\pi N}^{(3)} + \mathcal{L}_{\pi N}^{(4)} , \quad (41)$$

from which one calculates tree graphs with insertions from all terms $\mathcal{L}_{\pi N}^{(1,2,3,4)}$ and loop diagrams with at most one insertion from the dimension two operators collected in $\mathcal{L}_{\pi N}^{(2)}$. The lowest order effective Lagrangian contains g_A and m (note that the nucleon mass might be transformed into higher order $1/m$ corrections [88]). At order two, three and four one has 7, 23 and 118 LECs, respectively. While these numbers appear large,

it should be stressed that many of the dimension four operators contribute only to very exotic processes, like three or four pion production induced by photons or pions. Moreover, for a given process, it often happens that some of these operators appear in certain linear combinations and others simply amount to a quark mass renormalization of the corresponding dimension two operator. For example, in the case of elastic pion–nucleon scattering, one has 4, 5, and 4 independent LECs (or combinations) thereof at second, third and fourth order, respectively, which is a much smaller number than the total number of independent terms. Consequently, the often cited folklore that CHPT becomes useless beyond a certain order because the number of LECs increases drastically is not really correct. It is also important to stress that the values of the dimension two (and of some dimension three) LECs can be understood in terms of (low–lying) t –channel meson resonance and s –channel baryon resonance excitations [89] (the so–called resonance saturation). For further details, we refer the reader to references [82, 87].

3.4.2. Low–energy theorems for pion electroproduction We now wish to apply the machinery of baryon CHPT to the case of pion electroproduction and derive low–energy theorems (LETs). Before doing that, a few clarifying remarks about the meaning of such LETs are in order. Following the seminal work of Nambu *et al* [36, 37], pion electroproduction LETs have been discussed in the sixties, often using by now outdated methods, see [90, 91, 92, 93]. As already stressed, only using the methods of CHPT one can formulate model–independent statements beyond leading order, provided one is able to fix all LECs from data. The modern meaning of LETs is discussed in broad detail in reference [94]. To third order in the chiral expansion, the various isospin components of the transverse and the longitudinal S –wave multipoles can be written as functions of the two small parameters μ and ν , cf. equation (31), as (for details, see [74])

$$E_{0+}^{(+)}(\mu, \nu) = \frac{eg_{\pi N}}{32\pi m} \left\{ -2\mu + \mu^2(3 + \kappa_v) - \nu(1 + \kappa_v) + \frac{\mu^2 m^2}{4\pi^2 F_\pi^2} \Xi_1(-\nu\mu^{-2}) \right\} + \mathcal{O}(q^3), \quad (42)$$

$$L_{0+}^{(+)}(\mu, \nu) = E_{0+}^{(+)}(\mu, \nu) + \frac{eg_{\pi N}}{32\pi m} (\mu^2 - \nu) \left\{ \kappa_v + \frac{m^2}{4\pi^2 F_\pi^2} \Xi_2(-\nu\mu^{-2}) \right\} + \mathcal{O}(q^3), \quad (43)$$

$$E_{0+}^{(0)}(\mu, \nu) = \frac{eg_{\pi N}}{32\pi m} \left\{ -2\mu + \mu^2(3 + \kappa_s) - \nu(1 + \kappa_s) \right\} + \mathcal{O}(q^3), \quad (44)$$

$$L_{0+}^{(0)}(\mu, \nu) = E_{0+}^{(0)}(\mu, \nu) + \frac{eg_{\pi N}}{32\pi m} (\mu^2 - \nu) \kappa_s + \mathcal{O}(q^3), \quad (45)$$

$$E_{0+}^{(-)}(\mu, \nu) = \frac{eg_{\pi N}}{8\pi m} \left\{ 1 - \mu + C\mu^2 + \nu \left(\frac{\kappa_v}{4} + \frac{1}{8} + \frac{m^2}{6} \langle r_A^2 \rangle \right) + \frac{\mu^2 m^2}{8\pi^2 F_\pi^2} \Xi_3(-\nu\mu^{-2}) \right\} + \mathcal{O}(q^3), \quad (46)$$

$$L_{0+}^{(-)}(\mu, \nu) = E_{0+}^{(-)}(\mu, \nu) + \frac{eg_{\pi N}}{8\pi m} (\mu^2 - \nu) \left\{ \frac{\kappa_v}{4} + \frac{m^2}{6} \langle r_A^2 \rangle + \frac{\sqrt{(2 + \mu)^2 - \nu}}{2(1 + \mu)^{3/2}(\nu - 2\mu^2 - \mu^3)} + \left(\frac{1}{\nu - 2\mu^2} - \frac{1}{\nu} \right) (F_\pi^V(m^2\nu) - 1) + \frac{m^2}{8\pi^2 F_\pi^2} \Xi_4(-\nu\mu^{-2}) \right\} + \mathcal{O}(q^3), \quad (47)$$

with $\kappa_v = \kappa_p - \kappa_n = 3.71$ the isovector and $\kappa_s = \kappa_p + \kappa_n = -0.12$ isoscalar anomalous magnetic moment of the nucleon, $g_{\pi N}$ the strong pion–nucleon coupling constant (which

can be used instead of g_A by virtue of the Goldberger-Treiman relation) and $F_\pi^V(k^2)$ is vector (charge) form factor of the pion. The functions $\Xi_j(-\nu/\mu^2)$, ($j = 1, 2, 3, 4$) are given by

$$\begin{aligned}\Xi_1(\rho) &= \frac{\rho}{1+\rho} + \frac{(2+\rho)^2}{2(1+\rho)^{3/2}} \arccos \frac{-\rho}{2+\rho}, \\ \Xi_2(\rho) &= \frac{2-\rho}{(1+\rho)^2} - \frac{(2+\rho)^2-2}{2(1+\rho)^{5/2}} \arccos \frac{-\rho}{2+\rho}, \\ \Xi_3(\rho) &= \sqrt{1+\frac{4}{\rho}} \ln \left(\sqrt{1+\frac{\rho}{4}} + \frac{\sqrt{\rho}}{2} + 2 \int_0^1 \frac{\sqrt{(1-x)[1+x(1+\rho)]}}{x} \right. \\ &\quad \left. \times \arctan \frac{x}{\sqrt{(1-x)[1+x(1+\rho)]}} \right), \\ \Xi_4(\rho) &= \int_0^1 dx \frac{x(1-2x)}{\sqrt{(1-x)[1+x(1+\rho)]}} \arctan \frac{x}{\sqrt{(1-x)[1+x(1+\rho)]}}.\end{aligned}\quad (48)$$

These functions are shown in figure 6 for $0 < \rho < 10$. They exhibit a very smooth behavior. The influence of isospin breaking, i.e. the charged to neutral pion mass difference in the loops, has been discussed in reference [74], here it suffices to say that the ρ -dependence is only very little affected by such effects. Note that the LETs given

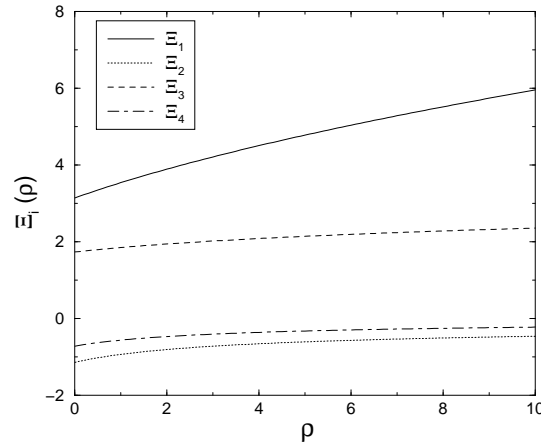


Figure 6. The functions $\Xi_i(\rho)$ ($i = 1, 2, 3, 4$) as defined in equations (48).

above do not contain the full electromagnetic form factors of the nucleon. This is due to the power counting of CHPT, from which one concludes that at third order one is only sensitive to the normalization of the magnetic form factors, i.e. the respective anomalous magnetic moments. At fourth order, one expects sensitivity to the electric charge radii of the proton and the neutron. Of particular interest are the LETs for the $(-)$ amplitudes because of the connection to the nucleon axial form factor, as will be discussed in the next paragraph. Here, we just mention that the constant C appearing in the expression for $E_{0+}^{(-)}$ can be expressed in terms of parameters that can be fixed in pion photoproduction, see [74]. Its explicit form is, however, not needed in what follows.

3.4.3. *Nucleon axial radius* From the LETs just given, we can now derive the relation between the electroproduction amplitude and the nucleon axial radius, following reference [95]. To separate the axial radius, one should consider the slope of the transverse multipole. For doing that, one has to expand the function $\Xi_3(-\nu\mu^{-2})$ in powers of $k^2 = \nu m^2$ and pick up all terms proportional to ν . However, to make the argument even clearer, we give one intermediate step. In fact, the direct diagrammatic evaluation of the electric dipole amplitude to third order in the chiral expansion includes the one-loop diagrams shown in figure 7. These lead to an additional contribution to

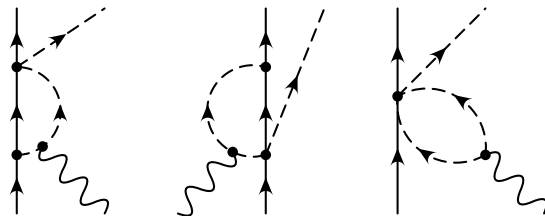


Figure 7. One-loop diagrams that lead to the axial radius correction. Crossed partners are not shown. The solid, dashed and wiggly lines denote nucleons, pions and photons, in order.

$E_{0+}^{(-)}$ at order k^2 that can not be obtained using current algebra methods,

$$E_{0+}^{(-)}(M_\pi \neq 0, k^2) = \frac{eg_A}{8\pi F_\pi} \left\{ 1 + \frac{k^2}{6} \langle r_A^2 \rangle + \frac{k^2}{4m^2} \left(\kappa_v + \frac{1}{2} \right) - \mu + C\mu^2 + \frac{\mu^2 m^2}{8\pi^2 F_\pi^2} \int_0^1 dx \int_0^x dy \ln \left[1 - x^2 + y^2 + \frac{\nu}{\mu^2} x(x-1) \right] \right\} + O(q^3). \quad (49)$$

Note that in a third order calculation, the electric dipole amplitude is only given to second order in small momenta. The constant C in (49) subsumes various k^2 -independent loop corrections together with contact terms and kinematical corrections of order $1/m^2$. In the chiral limit $\mu = 0$, one recovers of course the LET of Nambu *et al* [36, 37], because the last term of equation (49) vanishes identically at zero pion mass in the physical region $k^2 < 0$, compare also equation (36) and the discussion below. Matters are, however, different for non-vanishing pion mass, $\mu \neq 0$. Expanding the ln-term in (49) in powers of k^2 , the coefficient of the k^2 -term in equation (36) receives an extra contribution,

$$1 + \frac{k^2}{6} \langle r_A^2 \rangle + \frac{k^2}{4m} \left(\kappa_v + \frac{1}{2} \right) + \frac{k^2}{128F_\pi^2} \left(1 - \frac{12}{\pi^2} \right). \quad (50)$$

The last term in this equation constitutes a model-independent contribution at order k^2 not modified by higher loop or contact terms, which are suppressed by powers of μ . Formally, it appears because one cannot interchange the limits $M_\pi \rightarrow 0$ (chiral limit) and $k^2 \rightarrow 0$ (photon point). Therefore, what was believed to be the axial radius determined in pion electroproduction was nothing but the modified radius

$$\langle \hat{r}_A^2 \rangle = \langle r_A^2 \rangle + \frac{3}{64F_\pi^2} \left(1 - \frac{12}{\pi^2} \right). \quad (51)$$

The numerical value of this additional term is

$$\Delta\langle r_A^2 \rangle = \langle \tilde{r}_A^2 \rangle - \langle r_A^2 \rangle = -0.0456 \text{ fm}^2, \quad (52)$$

which translates into a shift of the axial mass of

$$\Delta M_A = 0.055 \text{ GeV}, \quad (53)$$

which is in agreement with the empirical value given in equation (11), $\Delta M_A = (0.043 \pm 0.026) \text{ GeV}$. This agreement can be considered as one of the premier successes of baryon chiral perturbation theory.

Since the lowest (third) order result for the axial radius discrepancy is quite small, one should investigate higher order corrections in μ to find out how reliable the leading order result is. This has been reported in [96] and we essentially follow the arguments given there. To order q^4 , which gives the pertinent next-to-next-to-leading order corrections, one has to consider one loop graphs with exactly one insertion from the dimension two πN Lagrangian and counterterms. The LECs related to these will be estimated from resonance exchange contributions, here ρ and Δ exchanges. Since we are only interested in the transverse part of the transition matrix element for $\gamma^*p \rightarrow \pi^+n$ at threshold, we introduce an auxiliary quantity $E(k^2)$, that is proportional to the transverse threshold S-wave multipole,

$$\mathbf{T} \cdot \boldsymbol{\epsilon} = \frac{ieg_A}{\sqrt{2}F_\pi} \boldsymbol{\sigma} \cdot \boldsymbol{\epsilon} E(k^2) = 4\pi i(1 + \mu) \boldsymbol{\sigma} \cdot \boldsymbol{\epsilon} E_{0^+, \text{thr}}^{\pi^+n}. \quad (54)$$

In the chiral limit, the corresponding current algebra result becomes exact and gives, when expanded in k^2

$$E(k^2) = 1 + \frac{k^2}{6} \langle \overset{\circ}{r}_A^2 \rangle - \frac{k^2}{2m} \left(\overset{\circ}{\kappa}_n + \frac{1}{4} \right) + \mathcal{O}(k^4), \quad (55)$$

with

$$\langle \overset{\circ}{r}_A^2 \rangle = \langle r_A^2 \rangle + \mathcal{O}(\mu^2), \quad \overset{\circ}{\kappa}_n = \kappa_n - \frac{g_A^2 m M_\pi}{8\pi F_\pi^2} + \mathcal{O}(\mu^2), \quad (56)$$

the nucleon axial radius and the neutron magnetic moment in the chiral limit. Here the superscript 'o' denotes quantities in the chiral limit, $\overset{\circ}{Q} = \overset{\circ}{Q} [1 + \mathcal{O}(m_{u,d})]$. Note that the axial radius (like the isocalar electromagnetic radius) is analytic in the quark masses. We now want to calculate all tree and loop graphs up to order q^4 which contribute to the slope $E'(0) = \partial E(0)/dk^2$ and are proportional to μ^0 and/or μ . The quantity $E'(0)$ is the sum of the desired squared axial radius and a host of other terms. Among these are contributions from the Born graphs including electromagnetic form factors. Since these are already contained in the standard analysis of the pion electroproduction data, such terms need not be considered further. The discrepancy subsumes all loop and counterterm effects which go beyond the form factors. After some lengthy calculation, one arrives at

$$\begin{aligned} \langle \tilde{r}_A^2 \rangle - \langle r_A^2 \rangle &= \frac{3}{64F_\pi^2} \left(1 - \frac{12}{\pi^2} \right) + \frac{3M_\pi}{64mF_\pi^2} + \frac{3c^+(\pi - 4)M_\pi}{32\pi F_\pi^2} \\ &+ \frac{3g_A^2 M_\pi}{8\pi^2 m F_\pi^2} \left(\ln \frac{M_\pi}{\lambda} - \frac{\pi^2}{16} + \frac{7\pi}{12} - \frac{1}{4} \right) + 6E'_\rho(0) + 6E'_\Delta(0). \end{aligned} \quad (57)$$

The first term in (57) is the leading order result already given before. The combination of LECs, $c^+ = -8c_1 + 4c_2 + 4c_3 - g_A^2/2m$, can be related to the isospin-even πN scattering length a_{0+}^+ via $c^+ = 8\pi F_\pi^2 a_{0+}^+ / M_\pi^2$ (which is correct to the order we are working here). The last two terms in (57) represent the counterterm contributions at order q^4 , which have been identified with $\rho(770)$ and $\Delta(1232)$ exchange contributions,

$$\begin{aligned} 6E'_\rho(0) &= -\frac{3(1 + \kappa_\rho)M_\pi}{16\pi^2 g_A m F_\pi^2}, \\ 6E'_\Delta(0) &= \frac{\kappa^* M_\pi}{\sqrt{2}m^2 m_\Delta^2} \left[\frac{m_\Delta^2 - m_\Delta m + m^2}{m_\Delta - m} \right. \\ &\quad \left. - 2m(Y + Z + 2YZ) - 2m_\Delta(Y + Z + 4YZ) \right], \end{aligned} \quad (58)$$

with $\kappa_\rho \simeq 6$ the tensor-to-vector ratio of the ρNN couplings and $\kappa^* = g_1 \simeq 5$ is the $\gamma\Delta N$ coupling constant. The so-called off-shell parameters Y and Z (which are nothing but higher order LECs in an effective field theory including the delta) have been constrained in reference [96] from the delta contribution to the proton's magnetic polarizability, $Y = -0.12$, and from the a_{33} πN scattering volume, $Z = -0.3$. Putting all pieces together, one finds for the axial radius discrepancy,

$$\langle \tilde{r}_A^2 \rangle - \langle r_A^2 \rangle = (-4.6 + 0.5) \cdot 10^{-2} \text{ fm}^2. \quad (59)$$

Note that there are large individual terms in the loop and the counterterm contributions which cancel each other. Also, this correction is fairly sensitive to the badly known isoscalar πN scattering length, so it is fair to assign an uncertainty to this correction which is as large as its central value given in equation (59). However, the only meaningful quantity is the total sum of all terms of order q^4 , which can also be considered verified by the MAMI experiment [24]. Taken that experiment face value, one could turn the argument around and give a bound on a_{0+}^+ . We refrain from doing that here but stress again the intricate interplay of seemingly unrelated processes, linked by the chiral structure of QCD. It should also be noted that the momentum transfers in the MAMI experiment were too high to allow for a direct and safe extraction of $E_{0+}^{(-)}$, therefore the data were analyzed in the framework of an effective Lagrangian model with the electromagnetic nucleon form factors, the pion vector form factor and the axial nucleon form factor at the appropriate vertices [97, 98]. A further measurement at lower energy and lower momentum transfer should therefore be studied for feasibility.

3.4.4. Pion charge radius The charge (vector) radius of the pion is a fundamental quantity in hadron physics. It can essentially be determined in two ways. One method is pion scattering off electrons (or electron-positron annihilation into pion pairs), this leads a pion root-mean-square (rms) radius of [99]

$$\langle r_\pi^2 \rangle_V^{1/2} = (0.663 \pm 0.006) \text{ fm}, \quad (60)$$

if one insists on the correct normalization of the pion charge (vector) form factor, $F_\pi^V(0) = 1$ (in units of the elementary charge e). A more recent determination of the

pion vector radius from low-momentum space- and time-like form factor data based on a very precise two-loop chiral perturbation theory representation [100] gives (two-loop contributions to the pion form factors were first considered in reference [101])

$$\langle r_\pi^2 \rangle_V^{1/2} = (0.661 \pm 0.012) \text{ fm} , \quad (61)$$

consistent with the value given above. Electromagnetic corrections considered in reference [102] reduce this value by about one percent. This number can be understood semi-quantitatively in a naive vector meson dominance picture, $\langle r_\pi^2 \rangle_V^{1/2} = \sqrt{6}/M_\rho \simeq 0.63 \text{ fm}$. The second method is based on charged pion electroproduction, $\gamma^* p \rightarrow \pi^+ n$. The unpolarized cross section in parallel kinematics decomposes into a transversal and a longitudinal piece, as detailed in section 3.4.2. While the former is sensitive to the the nucleon axial radius, the latter is quite sensitive to the pion form factor, i.e. to the pion radius for small momentum transfer. A recent measurement at the Mainz Microtron MAMI-II led to a pion radius of [24]

$$\langle r_\pi^2 \rangle_V^{1/2} = (0.74 \pm 0.03) \text{ fm} , \quad (62)$$

which is a sizeably larger value than the one obtained from πe scattering. It was hinted in reference [24] that their larger value for the pion radius might be due to the inevitable model-dependence based on the Born term approach to extract the pion radius. It was also stated that there might be an additional correction obtainable from chiral perturbation theory as it is the case for the nucleon axial radius discussed before. Indeed, there is such a similar kind of correction for the pion radius [105]. This new term modifies the momentum dependence of the longitudinal S-wave amplitude $L_{0+}^{(-)}$ and leads one to expect an even larger pion charge radius than the one given in equation (62). It is conceivable that higher order corrections yet to be calculated or contributions from higher multipoles will completely resolve the discrepancy between the pion radius determined from πe scattering on one side and from charged pion electroproduction on the other. Let us be more specific now. As shown in equation (47), the pion vector form factor $F_\pi^V(k^2)$ appears in the expression for the longitudinal multipole. The pion form factor has the following low-energy expansion,

$$F_\pi^V(k^2) = 1 + \frac{1}{6} \langle r_\pi^2 \rangle_V k^2 + \mathcal{O}(k^4) . \quad (63)$$

Consequently, to separate the pion radius, one should consider the slope of the longitudinal multipole. For doing that, one has to expand the function $\Xi_4(-\nu\mu^{-2})$ in powers of $k^2 = \nu m^2$ and pick up all terms proportional to ν . This gives:

$$\left. \frac{\partial L_{0+}^{(-)}}{\partial k^2} \right|_{k^2=0} = \frac{eg_{\pi N}}{32\pi m} \left\{ \frac{1}{M_\pi^2} - \frac{1}{mM_\pi} + \frac{13}{8m^2} + \frac{1}{3} \langle r_\pi^2 \rangle_V + \frac{1}{32F_\pi^2} \left(\frac{16}{\pi^2} - 1 \right) + \mathcal{O}(M_\pi) \right\} . \quad (64)$$

The first four terms are standard [106], they comprise the conventional dependence on the pion vector radius, recoil effects and the dominant chiral limit behavior of the slope of the longitudinal multipole. The strong $1/M_\pi^2$ chiral singularity stems from the k^2 -derivative of the pion-pole term which appears already at leading order in the chiral expansion (this is the leading contribution from the *induced pseudoscalar form*

factor). The last term in equation (64) originates from the so-called triangle and tadpole (with three pions coupling to the nucleon at one point) diagrams which are known to play a prominent role in pion photo- and electroproduction (see figure 7). The formal reason for the appearance of this new, model-independent contribution at order k^2 is that one cannot interchange the order of taking the derivative at $k^2 = 0$ and the chiral limit $M_\pi \rightarrow 0$. Consequently, all determinations of the pion radius from electroproduction (based on tree-level amplitudes including nucleon and pion form factors) have “measured” the modified radius,

$$\langle \tilde{r}_\pi^2 \rangle_V = \langle r_\pi^2 \rangle_V + \frac{3}{32F_\pi^2} \left(\frac{16}{\pi^2} - 1 \right). \quad (65)$$

The novel term on the right-hand-side of equation (65) amounts to 0.266 fm^2 , a bit more than half of the squared pion rms radius, $\langle r_\pi^2 \rangle_V \simeq 0.44 \text{ fm}^2$. Therefore, from the longitudinal multipole alone, one expects to find a larger pion radius if one analyses pion electroproduction based on Born terms,

$$\langle \tilde{r}_\pi^2 \rangle_V = (0.44 + 0.26) \text{ fm}^2 = (0.83 \text{ fm})^2, \quad (66)$$

which is even larger than the result of the Mainz analysis, cf. equation (62). We point out, however, that the contribution of the pion radius to the derivative of the longitudinal multipole is a factor of ten smaller than the one from the first three terms in the curly brackets in equation (64). Therefore, a fourth order analysis is certainly needed to further quantify the “pion radius discrepancy”. Furthermore, the pion form factor contribution to the longitudinal cross section is also present in higher multipoles. In fact, it is known that the convergence of the multipole series for the pion pole term is slow. One should therefore also investigate such effects for these higher multipoles or directly compare the predictions of complete one-loop calculation with the data of the longitudinal electroproduction cross section. For the purpose of demonstrating the significance of chiral loop effects the k^2 -slope is, however, best suited. What has been shown here is that as in the case of the nucleon axial mean square radius, the pion loops, which are a unique consequence of the chiral symmetry of QCD, modify the naive Born term analysis and should be taken into account.

4. Induced pseudoscalar form factor and coupling constant

4.1. QCD analysis of the induced pseudoscalar form factor

Here, we show that one can give an accurate prediction for the induced pseudoscalar form factor $G_P(t)$ and coupling constant g_P in terms of well-known physical parameters, following reference [107] (for a similar analysis, see [108]). For doing that, one exploits the chiral Ward identity of two-flavor QCD,

$$\partial^\mu \left(\bar{q} \gamma_\mu \gamma_5 \frac{\tau^a}{2} q \right) = \hat{m} \bar{q} i \gamma_5 \tau^a q \quad (67)$$

with \hat{m} the average light quark mass (note that isospin-breaking effects can be safely neglected here). Sandwiching equation (67) between nucleon states, one obtains [109]

$$mG_A(t) + \frac{t}{4m}G_P(t) = 2\hat{m}B \overset{\circ}{m} \overset{\circ}{g}_A \frac{1+h(t)}{M_\pi^2-t} \quad (68)$$

The pion pole in equation (68) originates from the direct coupling of the pseudoscalar density to the pion, $\langle 0|\bar{q}i\gamma_5\tau^a q|\pi^b\rangle = \delta^{ab}G_\pi$ [85]. The residue at the pion pole $t = M_\pi^2$ is [109]

$$\hat{m}G_\pi g_{\pi N} = g_{\pi N}F_\pi M_\pi^2 \quad (69)$$

with $g_{\pi N}$ the strong pion–nucleon coupling constant. The chiral expansion of the axial form factor and of the function $h(t)$ to order q^4 takes the form

$$G_A(t) = g_A \left(1 + \frac{\langle r_A^2 \rangle}{6}t \right), \quad h(t) = \text{const} - \frac{2\bar{d}_{18}}{g_A}t \quad (70)$$

with \bar{d}_{18} a low–energy constant (we use the notation of reference [110]) and one does not need to specify the constant since it is not needed explicitly in the following. The reason for the linear dependence in equation (70) is the following. The corresponding form factors $G_A(t)$ and $h(t)$ have a cut starting at $t = (3M_\pi)^2$ which in the chiral expansion first shows up at two–loop order $\mathcal{O}(q^5)$. Therefore, the contribution to order q^4 must be polynomial in t . Furthermore, from chiral counting it follows that the t^2 -terms are related to order q^5 of the full matrix–elements. Putting pieces together, we arrive at

$$m g_A + m g_A \frac{\langle r_A^2 \rangle}{6}t + \frac{t}{4m}G_P(t) = \frac{g_{\pi N}F_\pi}{M_\pi^2-t}t + g_{\pi N}F_\pi + \frac{2\bar{d}_{18}M_\pi^2 g_{\pi N}}{g_A} \quad (71)$$

using $2\hat{m}B \overset{\circ}{g}_A \overset{\circ}{m} = M_\pi^2(g_{\pi N}F_\pi + \mathcal{O}(M_\pi^2))$. At $t = 0$, equation (71) reduces to the Goldberger–Treiman discrepancy (GTD) [109, 111]

$$g_A m = g_{\pi N}F_\pi \left(1 + \frac{2\bar{d}_{18}}{g_A}M_\pi^2 \right), \quad (72)$$

which also clarifies the meaning of the low–energy constant \bar{d}_{18} . We will return to a more detailed discussion of the GTD in section 5. Finally, $G_P(t)$ can be isolated from equation (71),

$$G_P(t) = \frac{4m g_{\pi N}F_\pi}{M_\pi^2-t} - \frac{2}{3}g_A m^2 \langle r_A^2 \rangle + \mathcal{O}(t, M_\pi^2). \quad (73)$$

A few remarks are in order. First, notice that only physical and well–determined parameters enter in this formula. Second, while the first term on the right–hand–side is of order q^{-2} , the second one is $\mathcal{O}(q^0)$ and the corrections not calculated are of order q^2 . Third, the first term is the celebrated pion pole term, which stems from the direct coupling of the pion field to the pseudoscalar source. It clearly dominates this form factor for momentum transfers of the order of a few pion masses. Also, because of the pion pole, the structure of this form factor is not of the common form, i.e. its low–energy expansion is not a polynom characterized by some normalization and a radius.

Because of the Ward identities, it is linked to the axial form factor as witnessed by the appearance of the axial radius in equation (73). For the pseudoscalar coupling g_P , this leads to

$$g_P = \frac{2M_\mu g_{\pi N} F_\pi}{M_\pi^2 + 0.88M_\mu^2} - \frac{1}{3} g_A M_\mu m \langle r_A^2 \rangle . \quad (74)$$

Indeed, this relation has been derived long time ago by Adler and Dothan [112] and by Wolfenstein [113]. Wolfenstein used a once-subtracted dispersion relation for the right-hand-side of equation (68) (weak PCAC). It is gratifying that the ADW result can be firmly based on the systematic chiral expansion of low energy QCD Green functions. In chiral perturbation theory, one could in principle calculate the corrections to equation (74) by performing a two-loop calculation while in Wolfenstein's method these could only be estimated. To stress it again, the main ingredient to arrive at equation (74) in CHPT is the linear t -dependence in equation (70). Since we are interested here in a very small momentum transfer, like e.g. for the case of ordinary muon capture, $t = -0.88M_\mu^2 \simeq -0.5M_\pi^2$, curvature terms of order t^2 have to be negligible. If one uses for example the dipole parameterization for the axial form factor, the t^2 -term amounts to a 1.3% correction to the one linear in t . The masses m , M_μ and $M_\pi = M_{\pi^+}$ are accurately known and so are F_π and g_A [4]. The situation concerning the strong pion-nucleon coupling constant is less favorable. The methodologically best determination based on dispersion theory gave $g_{\pi N}^2/4\pi = 14.28 \pm 0.36$ [114], more recent determinations seem to favor smaller values [115]. We use here $g_{\pi N} = 13.10 \pm 0.35$. The value for the axial radius has been discussed in section 2.1, we use here the number obtained from neutrino scattering. Putting pieces together, we arrive at

$$g_P = (8.74 \pm 0.23) - (0.48 \pm 0.02) = 8.26 \pm 0.16 . \quad (75)$$

The uncertainties stem from the range of $g_{\pi N}$ and from the one for $\langle r_A^2 \rangle$ for the first and second term, in order. For the final result on g_P , we have added these uncertainties in quadrature. A measurement with a 2% accuracy of g_P , as intended by the upcoming experiment [55], could therefore cleanly separate between the pion pole contribution and the improved CHPT result. This would mean a significant progress in our understanding of this fundamental low-energy parameter since the presently available determinations have too large error bars to disentangle these values, see section 2.2. In fact, one might turn the argument around and eventually use a precise determination of g_P to get an additional determination of the strong pion-nucleon coupling constant which has been at the center of much controversy over the last years. To summarize, we have shown that the chiral Ward identities allow to predict the induced pseudoscalar coupling constant entirely in terms of well-determined physical parameters within a few percent accuracy. As already noted by Wolfenstein [113], an accurate empirical determination of this quantity therefore poses a stringent test on our understanding of the underlying dynamics which is believed to be realized in the effective low-energy field theory of QCD.

4.2. Chiral expansion of ordinary muon capture

As detailed in section 2.2, measurements of OMC on liquid hydrogen allow one to extract a value for the induced pseudoscalar coupling constant that agrees with theoretical expectations. The theoretical description of the hadronic physics involved is fairly transparent, we follow reference [116] and refer to that paper for many details. However, as stressed in particular by Ando, Myhrer and Kubodera [117], there are some difficulties with the accepted picture of translating the atomic rates into the one for liquid hydrogen. This topic will be taken up at the end of this section. First, we consider the OMC (atomic) decay rates calculated to third order in the chiral expansion and also to third order in the so-called ‘‘small scale expansion’’, which is an effective field theory with explicit $\Delta(1232)$ degrees of freedom (for a detailed introduction and review, see [118]). In the Fermi approximation of a static W_μ^- field, i.e. the gauge boson propagator is reduced to a point interaction (since the typical momenta involved are much smaller than the W mass),

$$\mathcal{M}_{\mu^-p \rightarrow \nu_\mu n} = \mathcal{M}^{\text{OMC}} = \langle \nu_\mu | W_\mu^+ | \mu \rangle i \frac{g^{\mu\nu}}{M_W^2} [\langle n | V_\nu^- | p \rangle - \langle n | A_\nu^- | p \rangle] , \quad (76)$$

where the vector current matrix element $\langle n | V_\nu^- | p \rangle$ (the so-called vector correlator) is parameterized in terms of the isovector vector Dirac and Pauli form factors $F_{1,2}^v$, which are known empirically (see e.g. [119, 120]) and have also been studied in baryon CHPT [111, 121, 122]. The axial correlator contains the desired dependence on the induced pseudoscalar form factor. Introducing the Fermi constant G_F , the square of the *spin-averaged* invariant matrix element is defined via

$$\frac{1}{4} \sum_{\sigma\sigma' ss'} |\mathcal{M}^{\text{OMC}}|^2 = \frac{1}{2} G_F^2 V_{ud}^2 L_{\mu\nu}^{(a)} H_{(a)}^{\mu\nu} . \quad (77)$$

with $V_{ud} = 0.974$ the pertinent CKM matrix element and the explicit forms of the symmetric leptonic $L_{\mu\nu}$, see also equation (16), and the hadronic tensor $H^{\mu\nu}$ are given in [116]. Approximating now the muonic atom wave-function dependence by its value at the origin (thus neglecting the small third order effects due to the form factors), the 1s Bohr wave function of the muonic atom reads

$$\Phi(0)_{1s} = \frac{\alpha^{3/2} \mu^{3/2}}{\sqrt{\pi}} , \quad (78)$$

with the reduced mass $\mu = (mM_{\mu^-})/(m + M_{\mu^-})$ and α the fine-structure constant. We can therefore calculate the spin-averaged rate of ordinary muon capture via

$$\Gamma_{\text{OMC}} = |\Phi(0)_{1s}|^2 \int \frac{d^3 r'}{(2\pi)^3 J_n} \frac{d^3 l'}{(2\pi)^3 J_\nu} (2\pi)^4 \delta^4(r + l - r' - l') \frac{1}{4} \sum_{\sigma\sigma' ss'} |\mathcal{M}^{\text{OMC}}|^2 \quad (79)$$

with J_ν, J_n appropriate normalization factors. Evaluating this to third order, $\mathcal{O}(q^3)$, one obtains

$$\Gamma_{\text{OMC}} = \left(\underbrace{247.0}_{\mathcal{O}(q)} \quad \underbrace{-61.6}_{\mathcal{O}(q^2)} \quad \underbrace{-3.8}_{\mathcal{O}(q^3)} + \mathcal{O}(1/m^3) \right) \times \text{s}^{-1} = 181.7 \times \text{s}^{-1} , \quad (80)$$

which shows a very fast convergence. Retaining the delta only reduces the small third order correction by 5%. The reason for the nice stability of perturbative calculations for OMC in the physical world of small finite quark masses is of course the fact that contributions of order n are suppressed by $(M_i/\Lambda_\chi)^{n-1}$, with $i = \pi, \mu$ and $\Lambda_\chi \sim m \sim 1$ GeV. This spin-averaged OMC scenario is mostly of theoretical interest. In nature the weak interactions show a very strong spin-dependence, which leads to quite different decay rates depending on whether the captured 1s muon forms a singlet or a triplet spin-state with the proton [123], where the singlet is the usual state $(1/\sqrt{2})(|\uparrow, \downarrow\rangle - |\downarrow, \uparrow\rangle)$ in terms of the muon and proton spins and the triplet accordingly, see also figure 3 and the discussion in section 2.2. Although the hyperfine splitting between the two levels “only” amounts to 0.04 eV, the occupation numbers of the levels due to thermal and collision induced processes tend to be far from statistical equilibrium. In order to make any contact with experiment, the singlet/triplet rates need to be calculated separately. For the total capture rates of singlet and the triplet states in the muonic atom, one find the following decomposition into leading, next-to-leading and next-to-next-to-leading order pieces

$$\begin{aligned}
 \Gamma_{\text{OMC}}^{\text{sing}} &= (957 - 245 \text{ GeV}/m + (30.4 \text{ GeV}/m^2 - 43.17) + \mathcal{O}(1/m^3)) \times \text{s}^{-1} \\
 &= 687.4 \times \text{s}^{-1} , \\
 \Gamma_{\text{OMC}}^{\text{trip}} &= (10.3 + 4.72 \text{ GeV}/m - (1.22 \text{ GeV}/m^2 + 1.00) + \mathcal{O}(1/m^3)) \times \text{s}^{-1} \\
 &= 12.9 \times \text{s}^{-1} ,
 \end{aligned} \tag{81}$$

displaying the dramatic spin-dependence due to the V-A structure of the weak interactions in the Standard Model. These numbers correspond to a value of $g_{\pi NN} = 13.05$ and include the pion pole corrections, cf. equation (74). Since G_P contributes negatively to the singlet rate a larger value of $g_{\pi NN}$ leads to a smaller value for the rate: $\Gamma_{\text{OMC}}^{\text{sing}} = 681.9 \times \text{s}^{-1}$ for $g_{\pi NN} = 13.4$. Similarly, neglecting the pion pole corrections leads to $\Gamma_{\text{OMC}}^{\text{sing}} = 676.1 \times \text{s}^{-1}$. In Equation (81) we have split the third order term (third and fourth terms in parenthesis) into the contribution from the $1/m^2$ corrections and the terms stemming from the various radii which lead to the Q^2 -dependence of the form factors. It is very interesting to note that these two contributions more or less cancels themselves in the case of the singlet term. It is thus extremely important to perform a consistent chiral expansion. The existing theoretical predictions for these rates are collected in table 2. For comparison, in a relativistic Born model one obtains the simple

Table 2. Calculated atomic singlet and triplet rates in s^{-1} from BHM [116], AMK [117], Primakoff [124] and Opat [123]. Note that the latter two have used smaller values for g_A and that AMK used $g_{\pi N} = 13.4$.

	BHM NLO	BHM NNLO	AMK NLO	AMK NNLO	Primakoff	Opat
Γ^{sing}	711	687.4	695	722	664 ± 20	634
Γ^{trip}	14.0	12.9	12.2	11.9	11.9 ± 0.7	13.3

nice formula for $\Gamma_{\text{OMC}}^{\text{sing}}$ [125]:

$$\begin{aligned} \Gamma_{\text{OMC}}^{\text{sing}} &\sim (6.236 F_1^v(q_0^2) + 0.5513 F_2^v(q_0^2) + 16.44 G_A(q_0^2) - 0.2834 G_P(q_0^2))^2 \\ &\sim 683 \times \text{s}^{-1} \end{aligned} \quad (82)$$

where $q_0^2 = -0.88M_\mu^2$ is the momentum transfer corresponding to muon capture at rest (again, a rescaling of this formula to the present day value of g_A has been performed). This formula though very appealing should not be used, being in contradiction with the modern viewpoint of power counting. The good agreement with the CHPT result is purely accidental. The problem arises from the fact that $\Gamma_{\text{OMC}}^{\text{sing}}$ is a rather sensitive quantity as can be seen for example in equation (82). Indeed the terms proportional to $F_2^v(q_0^2)$ and $G_P(q_0^2)$ are of the same order of magnitude but have different signs so they have a tendency to cancel each other rendering the values of Γ^{sing} rather sensitive to the exact values of these two quantities. So far we have only considered OMC for the case of muonic atoms. For the case of a liquid hydrogen target one also has to take into account the possibility of muon capture in a muonic molecule $p\mu p$, which can be formed via the reaction $p\mu + pep \rightarrow p\mu p + e + 124 \text{ eV}$. In such a molecule the muon can be found in the ortho (O) (spin of the protons parallel) or para (P) (spin of the protons antiparallel) spin state relative to its two accompanying protons. The decay rates of these molecular states can be calculated from the singlet/triplet rates of the muonic atom via

$$\Gamma_P = 2\gamma_P \frac{1}{4} (3\Gamma_{\text{trip}} + \Gamma_{\text{sing}}) , \quad (83)$$

$$\Gamma_O = p_{1/2} \Gamma_{1/2} + p_{3/2} \Gamma_{3/2} , \quad (84)$$

with γ_P (γ_O) denoting the ratio of the probability of finding the negative muon at the point occupied by a proton in the para-muonic (ortho-muonic) molecule and the probability of finding the negative muon at the origin in the muonic atom. The wavefunction corrections are taken to be $\gamma_O = 0.500$, $\gamma_P = 0.5733$ [126]. We note that the para molecular state is often referred to as the statistical mixture, as it corresponds to the naively expected occupation numbers of the muonic atom. For a precise calculation of the ortho molecular state on the other hand one first has to know the exact probabilities $p_{1/2}, p_{3/2}$ for the muonic molecule being in a total spin $S=(1-1/2)=1/2$ or a total spin $S=(1+1/2)=3/2$ state, with $p_{1/2} > 0.5$ [46], see also figure 3. The corresponding decay rates are given by [124, 46]

$$\begin{aligned} \Gamma_{1/2} &= 2\gamma_O \left(\frac{3}{4} \Gamma_{\text{sing}} + \frac{1}{4} \Gamma_{\text{trip}} \right) \\ \Gamma_{3/2} &= 2\gamma_O \Gamma_{\text{trip}} \end{aligned} \quad (85)$$

Theoretical calculations of the spin-effects in the muonic molecule [53] suggest $p_{1/2} \approx 1$, $p_{3/2} \approx 0$ which leads to the values:

$$\begin{aligned} \Gamma_P^{\text{OMC}} &= 208 \times \text{s}^{-1} \\ \Gamma_O^{\text{OMC}} &= 493 \dots 519 \times \text{s}^{-1} . \end{aligned} \quad (86)$$

where the range given in Γ_O^{OMC} corresponds to $0.95 \leq p_{1/2} \leq 1$. We have allowed here for a 5% uncertainty in the occupation numbers to show the sensitivity of our results on

this quantity. This point was first made in reference [117]. Since $\Gamma_{\text{sing}} \gg \Gamma_{\text{trip}}$ for OMC, $\Gamma_{\text{O}}^{\text{OMC}}$ turns out to be roughly proportional to $p_{1/2}$. We note that our number for capture from the molecular ortho state agrees very well with the most recent measurement $\Gamma_{\text{O}}^{\text{exp}} = (531 \pm 33) \times \text{s}^{-1}$ [52]. We stress again that a direct use of the liquid transition formula à la reference [53] is only meaningful if one accounts for the time structure of the beam in the experiment, see also [54].

4.3. Chiral expansion of radiative muon capture

The pioneering TRIUMF RMC result, cf. equation (15), spurred a lot of theoretical activity. While radiative muon capture had already been calculated in phenomenological tree level models a long time ago, see e.g. [64, 123, 127, 128, 129], heavy baryon chiral perturbation theory was also used at tree level including dimension two operators [130] and to one loop order [131]. The resulting photon spectra are not very different from the ones obtained in the phenomenological models, the most striking feature being the smallness of the chiral loops and polynomial third order corrections [131], hinting towards a good convergence of the chiral expansion. At present, the puzzling result from the TRIUMF experiment has not fully been explained, but it appears now that the discrepancy does not come only from the strong interactions but rather is also related to the distribution of the various spin states of the muonic atoms, as detailed below [116, 117]. It is therefore mandatory to sharpen the theoretical predictions for the strong as well as the non-strong physics entering the experimental analysis. Therefore, RMC was also analyzed in the framework of the small scale expansion [118], which allows to systematically include the Δ resonance into the effective field theory. Although Ando and Min [131] have already shown that the RMC process possesses a well behaved chiral expansion up to N^2LO , it has been noted quite early [132] that one should reanalyze RMC in a chiral effective field theory with explicit Δ degrees of freedom. This is due to the fact that the Δ -resonance lies quite close to the nucleon and therefore, in a delta-free theory like baryon CHPT, could lead to unnaturally large higher order contact interactions which would spoil the seemingly good chiral convergence. Stating this in the language of (naive) dimensional analysis, it suggests the possibility of corrections of the order of 30% due to the small nucleon–delta mass splitting, $M_{\mu}/(m_{\Delta} - m) \sim 3M_{\mu}/m$. Such a study including explicit delta degrees of freedom was performed in [116]. It should also be mentioned that phenomenological models have claimed for a long time that the Δ contribution does not exceed 8% in the photon spectrum for photon energies above 60 MeV [129]. We will now proceed to discuss general features of the chiral and the small scale expansion for RMC and then critically reexamine the way the TRIUMF experiment was analyzed.

4.3.1. General results In the static approximation for the W–boson, the pertinent matrix element for RMC decomposes into two terms,

$$\mathcal{M}_{\mu^- p \rightarrow \nu_{\mu} n \gamma} = \langle \nu_{\mu} | W_{\mu}^+ | \mu \rangle i \frac{g^{\mu\nu}}{M_W^2} [\langle n | \mathcal{T} V \cdot \epsilon^* V_{\nu}^- | p \rangle - \langle n | \mathcal{T} V \cdot \epsilon^* A_{\nu}^- | p \rangle]$$

$$+ \langle \nu_\mu \gamma | W_\mu^+ | \mu \rangle i \frac{g^{\mu\nu}}{M_W^2} [\langle n | V_\nu^- | p \rangle - \langle n | A_\nu^- | p \rangle] , \quad (87)$$

where the first one contains the vector–vector (VV) and vector–axial (VA) correlator. The hadronic part of the second term is, of course, identical to the OMC matrix–element. Following [116], we give these to second order in the chiral and the small scale expansion. The third order terms have been worked out by Ando and Min [131] and found to be small. Working in the Coulomb gauge for the photon and making use of the transversality condition $\epsilon^* \cdot k = 0$, one finds (the pertinent momenta were already given in equation (14))

$$\begin{aligned} \langle n | \mathcal{T} V \cdot \epsilon^* V_\mu^- | p \rangle^{(2)} &= -i \frac{g_2 V_{ud} e}{\sqrt{8}} \bar{n}(r') \left\{ \frac{1 + \kappa_v}{m} [S_\mu, S \cdot \epsilon^*] - \frac{1}{2m} \epsilon_\mu^* \right. \\ &\quad \left. + \frac{1}{m\omega} v_\mu [(1 + \kappa_v) [S \cdot \epsilon^*, S \cdot k] - \epsilon^* \cdot r] + \mathcal{O}(1/m^2) \right\} p(r) , \quad (88) \end{aligned}$$

$$\begin{aligned} \langle n | \mathcal{T} V \cdot \epsilon^* A_\mu^- | p \rangle^{(2)} &= -i \frac{g_2 V_{ud} e}{\sqrt{8}} \bar{n}(r') \times \\ &\quad \left\{ 2 R g_A \frac{S \cdot (r' - r)}{(r' - r)^2 - M_\pi^2} \times \left[\frac{2 \epsilon^* \cdot (l - l') (l - l')_\mu}{(l - l')^2 - M_\pi^2} - \epsilon_\mu^* \right] \right. \\ &\quad - R \frac{g_A}{m} \frac{(v \cdot r' - v \cdot r) S \cdot (r + r')}{(r' - r)^2 - M_\pi^2} \times \left[\frac{2 \epsilon^* \cdot (l - l') (l - l')_\mu}{(l - l')^2 - M_\pi^2} - \epsilon_\mu^* \right] \\ &\quad - 2 R g_A \left[1 + \frac{v \cdot l - v \cdot l'}{2m} \right] \frac{S \cdot \epsilon^* (l - l')_\mu}{(l - l')^2 - M_\pi^2} + \frac{g_A}{m} S \cdot \epsilon^* v_\mu \\ &\quad + \frac{g_A}{m} \left[\frac{(2 + \kappa_s + \kappa_v) S^\alpha [S \cdot \epsilon^*, S \cdot k]}{\omega} + \frac{(\kappa_v - \kappa_s) [S \cdot \epsilon^*, S \cdot k] S^\alpha}{\omega} \right. \\ &\quad \left. - \frac{2 S^\alpha \epsilon^* \cdot r}{\omega} \right] \times \left[g_{\mu\alpha} - R \frac{(l - l')_\alpha (l - l')_\mu}{(l - l')^2 - M_\pi^2} \right] \\ &\quad + \frac{g_{\pi N \Delta} b_1}{3m} \left[\frac{2\Delta [k^\alpha S \cdot \epsilon^* - \omega v^\alpha S \cdot \epsilon^* - \epsilon^{*\alpha} S \cdot k]}{\Delta^2 - \omega^2} - \frac{4 S^\alpha [S \cdot \epsilon^*, S \cdot k]}{3(\Delta + \omega)} \right. \\ &\quad \left. + \frac{4 [S \cdot \epsilon^*, S \cdot k] S^\alpha}{3(\Delta - \omega)} \right] \times \left[g_{\mu\alpha} - \frac{(l - l')_\alpha (l - l')_\mu}{(l - l')^2 - M_\pi^2} \right] + \mathcal{O}(1/m^2) \left. \right\} p(r) , \quad (89) \end{aligned}$$

with $\omega = v \cdot k$, S^μ the covariant nucleon spin–vector, v_μ the nucleons four–velocity (see e.g. reference [111] for a more detailed discussion of the underlying heavy baryon formalism) and $R = 1$ in QCD. Furthermore, κ_s is the nucleon isoscalar anomalous magnetic moment, $\Delta = m_\Delta - m$ the delta–nucleon mass splitting, $g_{\pi N \Delta}$ and b_1 are the leading $\pi N \Delta$ and $\gamma N \Delta$ coupling constants. Numerically, $g_{\pi N \Delta} \times b_1 = 1.05 \times 12 = 12.6$ [118]. The SU(2) gauge coupling g_2 is related to the Fermi constant via $G_F = g_2^2 \sqrt{2} / (8M_W^2)$. Note that the vector–vector correlator is free of delta effects at next–to–leading order, i.e. the leading $\Delta(1232)$ effect only appears in the vector–axial correlator. The latter terms constitute the difference between the chiral and the small scale expansions for RMC evaluated to NLO. The factor R multiplying the Born term contributions proportional to the induced pseudoscalar form factor has been introduced

for the later discussion. Note again that these expressions do not contain the full form factor $G_P(t)$ but only its leading part (the CHPT correction given in equation (73) does not appear at this order). One can easily check from the continuity equations satisfied by the correlators that gauge invariance is satisfied in the above equations. We are now in the position to calculate the decay rates. Consider first the spin-averaged case. The square of the matrix-element equation (87) can be written as a sum of four terms, with both photons coming either from the hadronic or the leptonic side and two mixed terms, i.e.

$$\frac{1}{4} \sum_{\sigma\sigma's's'\lambda\lambda'} |\mathcal{M}^{\text{RMC}}|^2 = \frac{e^2 G_F^2 V_{ud}^2}{2} \left[L_{\mu\nu}^{(a)} H_{(d)}^{\mu\nu} + \left(\sum_{\lambda\lambda'} L_{\mu\nu}^{(b)} H_{(c)}^{\mu\nu} + L_{\mu\nu}^{(c)} H_{(b)}^{\mu\nu} \right) + L_{\mu\nu}^{(d)} H_{(a)}^{\mu\nu} \right], \quad (90)$$

with λ, λ' the photon helicities. Explicit expressions for the various tensors are not given here because they are lengthy and not illuminating. The total decay rate is given by:

$$\Gamma_{\text{tot}} = \frac{|\Phi(0)_{1s}|^2}{16\pi^4} \int_0^\pi \sin\theta d\theta \int_0^{\omega_{\text{max}}} d\omega \omega l'_0 \left(1 - \left(\frac{m_\mu - \omega(1 - \cos\theta)}{m} \right) \right) \times \frac{1}{4} \sum_{\sigma\sigma's's'\lambda\lambda'} |\mathcal{M}^{\text{RMC}}|^2, \quad (91)$$

with $\omega = k_0$ the photon energy (note that in this and the following subsection we exceptionally use the symbol ω for the photon energy to facilitate the comparison with the literature). The direction of the photon defines the z-direction and θ in equation (91) is the polar angle of the outgoing lepton with respect to this direction. The maximal photon energy is given by

$$\omega_{\text{max}} = M_\mu \left(1 + \frac{M_\mu}{2m} \right) \left(1 + \frac{M_\mu}{m} \right)^{-1}. \quad (92)$$

Furthermore, the energy of the outgoing lepton follows from energy conservation,

$$l'_0 = M_\mu - \omega - \frac{M_\mu^2}{m} + \frac{\omega(1 - \cos\theta)(M_\mu - \omega)}{m} + \mathcal{O}(1/m^2). \quad (93)$$

First we discuss the (academic) spin-averaged RMC scenario, which allows for a comparison with previous calculations:

$$\begin{aligned} \Gamma_{\text{spinav.}}^{\text{RMC}} &= (66.0 + 18.7 + \mathcal{O}(1/m^2)) \times 10^{-3} \text{ s}^{-1} = 84.7 \times 10^{-3} \text{ s}^{-1} \text{ (CHPT)} \\ \Gamma_{\text{spinav.}}^{\text{RMC}} &= (66.0 + 20.4 + \mathcal{O}(1/m^2)) \times 10^{-3} \text{ s}^{-1} = 86.4 \times 10^{-3} \text{ s}^{-1} \text{ (SSE)}. \end{aligned} \quad (94)$$

Both the CHPT and the SSE results suggest a good convergence for the chiral expansion, as expected from dimensional analysis. Note that the leading order capture rates in both calculations are identical, as $\Delta(1232)$ related effects only start at sub-leading order. Our leading order result also agrees with the calculation of reference [130]. For the case of muonic atoms we obtain the following decay rates in the singlet/triplet channel (note the reversal of the relative size of the singlet to triplet contribution as compared to the OMC case),

$$\begin{aligned} \Gamma_{\text{sing}}^{\text{RMC}} &= (12.7 - 18.7 \text{ GeV}/m + \mathcal{O}(1/m^2)) \times 10^{-3} \text{ s}^{-1} = 3.10 \times 10^{-3} \text{ s}^{-1} \text{ (CHPT)} \\ \Gamma_{\text{sing}}^{\text{RMC}} &= (12.7 - 18.3 \text{ GeV}/m + \mathcal{O}(1/m^2)) \times 10^{-3} \text{ s}^{-1} = 2.90 \times 10^{-3} \text{ s}^{-1} \text{ (SSE)} \end{aligned}$$

$$\begin{aligned}\Gamma_{\text{trip}}^{\text{RMC}} &= (119 - 3.86 \text{ GeV}/m + \mathcal{O}(1/m^2)) \times 10^{-3} \text{ s}^{-1} = 112 \times 10^{-3} \text{ s}^{-1} \text{ (CHPT)} \\ \Gamma_{\text{trip}}^{\text{RMC}} &= (119 - 1.80 \text{ GeV}/m + \mathcal{O}(1/m^2)) \times 10^{-3} \text{ s}^{-1} = 114 \times 10^{-3} \text{ s}^{-1} \text{ (SSE)}\end{aligned}\quad (95)$$

It should be stressed that for the total numbers given the kinematical factors were not expanded in powers of $1/m$ since in case of the small singlet, the contribution from the terms starting at order $1/m^2$ can not be neglected. Next, we address the complications for RMC due to the presence of muonic molecules in the liquid hydrogen target. According to equation (83), we can easily determine the capture rate from the molecular para state

$$\Gamma_P^{\text{RMC}} = 85.2 [86.4] \times 10^{-3} \text{ s}^{-1} \text{ (CHPT [SSE])} . \quad (96)$$

Consider now the molecular ortho state, which turns out to dominate in the recent RMC experiment from TRIUMF [62, 63]. One obtains for $p_{1/2} = 1$:

$$\Gamma_O^{\text{RMC}} = 30.4 [30.8] \times 10^{-3} \text{ s}^{-1} \text{ (CHPT [SSE])} , \quad (97)$$

i.e in both cases the delta effects are fairly small. Due to the triplet dominance in RMC (as opposed to the singlet dominance in OMC) Γ_O^{RMC} is now roughly proportional to $(1 - 3/4p_{1/2})$ which leads to a big sensitivity of the RMC capture rate to the exact occupation numbers of the relative molecular sub-states. For example, a 5% uncertainty in the occupation numbers $p_{1/2} = 0.95$, $p_{3/2} = 0.05$ would lead to a 13% change in the ortho capture rate $\Gamma_O^{\text{RMC}} \sim 35 \times 10^{-3} \text{ s}^{-1}$. We will discuss the implications of this uncertainty when we compare our results with the measured photon spectrum from TRIUMF in the next subsection. For the total capture rate in the TRIUMF experiment

$$\Gamma_{\text{RMC}}^{H_2} = f_S \Gamma_{\text{sing}}^{\text{RMC}} + f_O \Gamma_O^{\text{RMC}} + f_P \Gamma_P^{\text{RMC}} \quad (98)$$

with $f_S = 0.061$, $f_O = 0.854$, $f_P = 0.085$ [62, 63] one would obtain $\Gamma_{\text{RMC}}^{\text{TRIUMF}} = (34.3 [34.8] + \mathcal{O}(1/m^2)) \times 10^{-3} \text{ s}^{-1}$ in HBCHPT [SSE]. This leads to a relative branching ratio $Q_\gamma = \Gamma_{\text{RMC}}/\Gamma_{\text{OMC}}$

$$Q_\gamma = 6.8 [6.9] \times 10^{-5} + \mathcal{O}(1/m^2) \text{ (CHPT [SSE])} . \quad (99)$$

Unfortunately the full relative branching ratio is not accessible in experiment, as one has to use a severe cut on the photon energies due to strong backgrounds. In the TRIUMF experiment only photons with an energy $\omega > 60 \text{ MeV}$ were detected. We therefore now move on to a discussion of the photon spectrum $d\Gamma/d\omega$. It can be obtained straightforwardly from equation (91). The calculated photon spectra to second order in CHPT and SSE come out very similar. In figure 8 we show the second order SSE results for the singlet, triplet, para and ortho states. The relative difference between the second order CHPT and SSE calculation for all states are of the order of a few percent, showing explicitly the small role of $\Delta(1232)$ in RMC. These results are very similar to the ones found by Beder and Fearing [64, 129] for the spectra and the relative contribution from the spin-3/2 resonance, although their calculation is based on a very different approach. Even the result for the small singlet is comparable though not identical to the one of Beder and Fearing. We conclude that the strong interaction theory for RMC is under control.

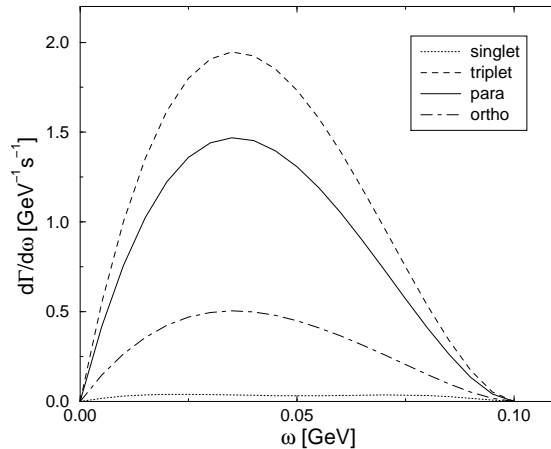


Figure 8. Photon spectra for RMC for the singlet, triplet, para (statistical) and ortho states of the $\mu - p$ system calculated to second order in the small scale expansion.

4.3.2. Discussion of the TRIUMF result The photon spectra just discussed allow in principle to determine the induced pseudoscalar form factor. The TRIUMF result for g_P is obtained by multiplying the terms proportional to the pseudoscalar form factor with a constant denoted R (the momentum dependence is assumed to be entirely given by the pion pole). The value of R is then extracted using the model of Fearing *et al* to match the partial rate for photon energies larger than 60 MeV. If we perform such a procedure, we get a similar shift in the partial photon spectra. It is, however, obvious from the analysis presented above that such a procedure is not legitimate. By artificially enhancing the contribution $\sim g_P$ (to simulate this procedure, we have introduced the factor R in equation (89) and similarly one must multiply $\langle n | A_\mu^- | p \rangle$ by R), one mocks up a whole class of new contact and other terms not present in the Born term model. To demonstrate these points in a more quantitative fashion, we show in figure 9 the partial branching fraction in comparison to the one with g_P enhanced by a factor 1.5 and a third curve, which is obtained by increasing g_P only by 15% and slightly modifying some parameters related to the delta contribution. This is shown by the dashed line and it shows that such a combination of small effects can explain most (but not all) of the shift in the spectrum. This is further sharpened by using now the neutral pion mass of 134.97 MeV instead of the charged pion mass, leading to the dotted curve in figure 9. Since the pion mass difference is almost entirely of electromagnetic origin, one might speculate that isospin-breaking effects should not be neglected. Furthermore, as discussed above a slight change in the occupation numbers $p_{1/2}$ and $p_{3/2}$ would also lead to an increase in the ortho capture rate which could close the gap between the empirical and theoretical results. For example the dashed curve in figure 9 would be moved from 0.42 to 0.48 while the dotted one would go from 0.50 to 0.54 with $p_{1/2} = 0.95$ and $p_{3/2} = 0.05$ at $\omega = 60$ MeV. The situation is reminiscent of the sigma term analysis, where many small effects combine to give the sizeable difference between the sigma term at zero momentum transfer and at the Cheng-Dashen point. Another point against the

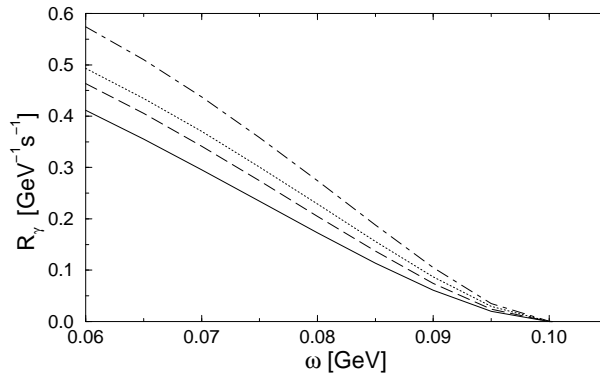


Figure 9. Photon spectra for RMC for the branching ratios of the singlet, ortho and para states as used in the TRIUMF analysis. Solid line: Prediction of the small scale expansion to order ϵ^2 . Dash-dotted line: Same as the solid line but with g_P scaled by a factor 1.5. Dashed line: Various small modifications as explained in the text. Dotted line: Same as the dashed line but using the neutral instead of the charged pion mass.

simple rescaling comes from OMC. Indeed if this rescaling holds for RMC it should also hold for OMC. We thus have performed a similar calculation in OMC. Taking the same value for R , one would obtain

$$\Gamma_{\text{OMC}}^{R=1.5} = 172.8 \times \text{s}^{-1}, \quad \Gamma_{\text{OMC}}^{\text{sing}, R=1.5} = 634.6 \times \text{s}^{-1}, \quad \Gamma_{\text{OMC}}^{\text{trip}, R=1.5} = 18.9 \times \text{s}^{-1}, \quad (100)$$

leading to $\Gamma_{\text{O}}^{\text{OMC}, R=1.5} = 477 \times \text{s}^{-1}$, which is lower than the error bars of the experimental result from reference [52]. As expected, the singlet and triplet capture rates are much more sensitive to the details of the interaction than the total rate. As a conclusion we note that the effect of enhancing the capture rates in RMC via setting $R = 1.5$ leads to a strong reduction of the corresponding OMC rates leading to conflicts with the experimentally determined ortho capture rate. To summarize this discussion, we have pointed out that two effects in particular have to be investigated in more detail: (1) the occupation numbers of the atomic structure in muonic atoms/molecules need to be carefully re-examined, and (2) the N²LO calculation should be redone including all isospin breaking effects because of the sensitivity to the exact pion mass in the pion-pole contributions, for example. The sum of these small effects should explain the observed photon spectrum, as we believe that the proper hadronic/weak physics part is well under control by now. A simple rescaling of the pseudoscalar coupling constant should no longer be considered.

5. Octet Goldberger-Treiman discrepancies

In section 4 we already encountered the Goldberger-Treiman discrepancy (GTD), i.e. the deviation from the Goldberger-Treiman relation (GTR), which is exact in the chiral limit. This deviation is parameterized in terms of the quantity Δ_π given by

$$\Delta_\pi = 1 - \frac{m g_A}{F_\pi g_{\pi NN}(M_\pi^2)} = 1 - \frac{g_{\pi NN}(0)}{g_{\pi NN}(M_\pi^2)}, \quad (101)$$

using the GTR $m g_A(0) = F_\pi g_{\pi NN}(0)$. Inserting the PDG values for g_A , F_π and $m = (m_p + m_n)/2$, one obtains

$$\Delta_\pi = 0.014 (0.040) \quad \text{for } g_{\pi NN} = 13.05 (13.40) . \quad (102)$$

From naive dimensional analysis one can estimate $\Delta_\pi \simeq (M_\pi/\Lambda_\chi)^2 = (M_\pi/4\pi F_\pi)^2 \simeq 0.015$, so this favors the smaller pion–nucleon coupling constant. Note, however, that if one chooses the ρ –meson mass as the relevant hadronic scale, $\Lambda_\chi = M_\rho$, this estimate increases to $(M_\pi/M_\rho)^2 \simeq 0.033$. One can further sharpen this argument by extending the analysis to flavor SU(3) and also investigate consistency of the strange to light quark mass ratio as obtained from the Goldstone boson spectrum. This is based on the observation that while in SU(2) the GTD is given in terms of one LEC, in chiral SU(3) this quantity is given in terms of a sum of quark masses times an SU(3) octet operator. This leads to a relation between various GTDs in the octet, the so–called Dashen–Weinstein relation [133]. This can be explored more systematically in the framework of CHPT. We follow here essentially reference [134] and the recent update given in [135] (see also [136]). In the baryon octet, one calculates matrix–elements of the axial–currents $\bar{u}\gamma_\mu\gamma_5 d$ and $\bar{u}\gamma_\mu\gamma_5 s$ at zero momentum transfer,

$$\langle B'(p)|A_\mu|B(p)\rangle = \bar{u}_{B'} \left[g_A^{B'B} \gamma_\mu\gamma_5 + \dots \right] u_B , \quad (103)$$

and the pertinent axial coupling constants $g_A^{B'B}$ can be measured in semi–leptonic hyperon decays (β –decays), $B \rightarrow B'\ell\nu_\ell$. Extending the analysis of section 4 to the SU(3) case, one can derive a variety of GTR’s and the chiral corrections to these. We focus here on the three cases for which sufficient empirical information for the corresponding strong meson–baryon coupling constants is available, i.e. np , Λp and $\Sigma^- n$ transitions. To linear order in the quark masses, the chiral Ward identity relating the divergence of the axial current to the pseudoscalar density sandwiched between baryon states leads to

$$\begin{aligned} (m_n + m_p)g_A^{np} &= 2F_\pi g_{\pi NN} + (m_u + m_d)H^{np}(0) + \text{O}(m_q^2) , \\ (m_\Lambda + m_p)g_A^{\Lambda p} &= -\sqrt{2}F_K g_\Lambda + (m_u + m_s)H^{\Lambda p}(0) + \text{O}(m_q^2) , \\ (m_{\Sigma^-} + m_n)g_A^{\Sigma^- n} &= 2F_K g_\Sigma + (m_u + m_s)H^{\Sigma^- n}(0) + \text{O}(m_q^2) , \end{aligned} \quad (104)$$

with $g_\Lambda = -g_{\Lambda p K^-}$ and $g_\Sigma = g_{\Sigma^- n K^-}/\sqrt{2}$. Furthermore, the functions $H^{BB'}(t)$ are SU(3) generalizations of $h(t)$ in equation (68), given by

$$\begin{aligned} \langle p|\bar{u}i\gamma_5 d|n\rangle &= [H^{np}(t) + \pi - \text{pole}] \bar{u}_p i\gamma_5 u_n , \\ \langle p|\bar{u}i\gamma_5 s|\Lambda\rangle &= [H^{\Lambda p}(t) + K - \text{pole}] \bar{u}_p i\gamma_5 u_\Lambda , \\ \langle n|\bar{u}i\gamma_5 s|\Sigma^-\rangle &= [H^{\Sigma^- n}(t) + K - \text{pole}] \bar{u}_n i\gamma_5 u_{\Sigma^-} . \end{aligned} \quad (105)$$

Note that we are using the convention for the axial charges so that g_A^{np} is positive. The H functions admit a chiral expansion,

$$\begin{aligned} H^{np}(0) &= F + D + \text{O}(m_q) , \\ H^{\Lambda p}(0) &= -\sqrt{\frac{2}{3}} \left(F + \frac{1}{3}D \right) + \text{O}(m_q) , \\ H^{\Sigma^- n}(0) &= -F + D + \text{O}(m_q) . \end{aligned} \quad (106)$$

Here, $F = 0.46$ and $D = 0.80$ are SU(3) axial–vector couplings. Therefore we have three relations with two unknowns, from that we can deduce a sum rule in terms of the GTD’s ($\Delta_\pi, \Delta_K^\Lambda, \Delta_K^\Sigma$) and the quark masses, sometimes called the Dashen–Weinstein relation (DWR),

$$\Delta_\pi = \frac{F_K}{F_\pi} \frac{\hat{m}}{\hat{m} + m_s} \left(\sqrt{3} \frac{g_{K\Lambda N}}{g_{\pi NN}} \Delta_K^\Lambda + \frac{g_{K\Sigma N}}{g_{\pi NN}} \Delta_K^\Sigma \right), \quad (107)$$

in terms of the kaon discrepancies $\Delta_K^{\Lambda, \Sigma}$,

$$\begin{aligned} \Delta_K^\Lambda &= 1 - \frac{\sqrt{3}(m_p + m_\Lambda) g_A^{\Lambda p}(0)}{2 F_K g_{K\Lambda N}(M_K^2)}, \\ \Delta_K^\Sigma &= 1 - \frac{(m_n + m_{\Sigma^-}) (-g_A^{\Sigma^- n}(0))}{2 F_K g_{K\Sigma N}(M_K^2)}. \end{aligned} \quad (108)$$

and $\hat{m} = (m_u + m_d)/2$ the average light quark mass. There are two ways to explore the DWR. First, consider the quark mass ratio appearing in equation (107) known, $2\hat{m}/(\hat{m} + m_s) = M_\pi^2/M_K^2 \simeq 0.08$. Note that higher order strong as well as electromagnetic corrections do not change this leading order estimate appreciably, see e.g. [137]. Then one can ask the question whether three GTDs are mutually consistent, that is whether the DWR is fulfilled. Another way of exploring this relation is to determine the three discrepancies from data and then use the DWR to deduce the quark mass ratio $\hat{m}/(\hat{m} + m_s)$. As input, we use the PDG values for the masses and axial coupling constants together with $g_{K\Lambda N}(M_K^2) = 13.7 \pm 0.4$ and $g_{K\Sigma N}(M_K^2) = 3.9 \pm 0.4$ as obtained from the analysis of hyperon–antihyperon production at LEAR [138]. These numbers are close to the expectations from flavor SU(3), $g_{K\Lambda N} = 13.5$ and $g_{K\Sigma N} = 4.3$, respectively, and in rough agreement with the analysis of $\bar{K}N$ scattering data given in reference [139]. This leads to the following values of the kaon discrepancies

$$\Delta_K^\Lambda = 0.16 \pm 0.06, \quad \Delta_K^\Sigma = 0.18 \pm 0.11. \quad (109)$$

These numbers conform to the expectations from SU(3) symmetry breaking, $\Delta_K \simeq (M_K/\Lambda_\chi)^2 = 0.18$, but the theoretical uncertainties might be larger as the ones given, see the discussion at the end of this section. Using now the quark mass ratio as deduced from the Goldstone boson masses and the central values of the GTDs, one obtains $\Delta_\pi = 0.016$, which favors the low value of the pion–nucleon coupling constant. If, on the other hand, one uses the empirical values of the GTDs, see equations (102,109), one obtains for the quark mass ratio

$$\frac{m_s}{\hat{m}} = \begin{cases} 22.4 \pm 6.8 & \text{for } g_{\pi NN} = 13.05 \\ 7.4 \pm 3.3 & \text{for } g_{\pi NN} = 13.40 \end{cases}, \quad (110)$$

i.e. the smaller value of $g_{\pi NN}$ is consistent with the standard scenario of chiral symmetry breaking, that is a large value of the quark condensate, $B = \langle 0|\bar{q}q|0\rangle/F_\pi^2 \simeq 1.5 \text{ GeV}$. One could be content with this consistency since the so determined quark mass ratio is in good agreement with the one obtained from analyzing the Goldstone boson mass spectrum based on the large condensate scenario. However, as already stressed in [134], a

better and more reliable determination of the strong coupling constants $g_{K\Lambda N}$ and $g_{K\Sigma N}$ is called for. In this context it is worth to stress that extraction of these couplings from kaon electroproduction data usually leads to very different values, see e.g. [140] and the discussion in reference [141]. Note, however, that most of these kaon electroproduction analyses are based on simple Born terms (including resonance excitations and form factors) and are therefore plagued with large theoretical uncertainties. In the light of the new and coming data on kaon electroproduction off protons and deuterium from ELSA and CEBAF, it would be very valuable to apply the theoretical framework of references [142, 143], which combines chiral perturbation theory, unitarity and coupled channel dynamics (see also [144, 145]). The presently existing uncertainties for these coupling constants inhibit a precise test of the chiral symmetry breaking pattern of QCD.

6. Summary and outlook

The nucleon as probed with the weak axial current can be parameterized in terms of two form factors, the axial, $G_A(t)$, and the induced pseudoscalar, $G_P(t)$, one. In this short review, we have shown that precise theoretical methods based on the symmetries of QCD exist for extracting these fundamental observables from experiment. The axial form factor can be well described by a dipole, $G_A(t) = (1 - t/M_A^2)^{-2}$. The dipole mass M_A can be translated into an axial root-mean-square radius of $\langle r_A^2 \rangle^{1/2} = 0.67 \pm 0.01$ fm. This value is consistently obtained from (anti)neutrino scattering off protons (or light nuclei) and charged pion electroproduction off protons. Clearly, more precise electroproduction data in the threshold region would be welcome to further pin down this quantity. The induced pseudoscalar form factor is dominated by the pion pole, but the small corrections to this leading order result have been calculated. Existing data from ordinary muon capture are consistent with these theoretical expectations but have too large error bars to cleanly test the chiral dynamics of QCD. We have argued that the result of the pioneering TRIUMF radiative muon capture experiment should be taken *cum grano salis* due to some assumptions in the analysis that are inconsistent with the power counting underlying the effective field theory of the Standard Model. However, it is fair to say that more theoretical as well as experimental effort is needed for drawing a final conclusion. The momentum-dependence of the induced pseudoscalar form factor is dominated by the pion pole which has only been tested in one electroproduction experiment so far. Also, a better determination of strong kaon-hyperon-nucleon coupling constants $g_{K\Lambda N}$ and $g_{K\Sigma N}$ would allow for an additional stringent bound on the light to strange quark mass ratio, based on the derivations from the octet Goldberger-Treiman relations. All this shows that precision experiments in hadron and nuclear physics indeed help to unravel the mysteries of QCD at energies where one really has to deal with *strong* interactions. Therefore, more pion and kaon electroproduction as well as muon capture experiments are called for.

Acknowledgments

We are grateful to Norbert Kaiser and Thomas Hemmert for fruitful collaborations, Fred Myhrer for sharing his insight into the theory of muon capture and Simon Širca for detailed explanation of the MAMI data and analysis. Useful communications from Barry Holstein, Jacques Martino and Claude Petitjean are acknowledged. We thank Josef Speth for initiating this project. We also thank the Deutsche Forschungsgemeinschaft and the ELSA/MAMI Schwerpunktprogramm for funding the workshop on “Hadron Form Factors” in Bad Honnef in April 2001, which triggered this write-up. This work was supported in part by the NSF, grant 34201.

References

- [1] Ulf-G. Meißner, Phys. Rept. 161 (1988) 213.
- [2] S. Weinberg, Phys. Rev. 112 (1958) 1375.
- [3] M. Morita, R. Morita and K. Koshigiri, Nucl. Phys. A577 (1994) 387c.
- [4] D.E. Groom *et al* (Particle Data Group), Eur. Phys. J. C5 (2000) 1.
- [5] J. Reich *et al* , Nucl. Inst. Meth. A440 (2000) 535.
- [6] H. Abele, Nucl. Inst. Meth. A440 (2000) 499.
- [7] I.S. Towner and J.C. Hardy, in *Symmetries and Fundamental Interactions in Nuclei*, E.M. Henley and W.C. Haxton (eds.) (World Scientific, Singapore, 1995), pp. 183-249.
- [8] G. Fanourakis *et al* , Phys. Rev. D21 (1980) 562.
- [9] L. A. Ahrens *et al* , Phys. Rev. D35 (1987) 785.
- [10] L. A. Ahrens *et al* , Phys. Lett. B202 (1988) 284.
- [11] S. J. Barish *et al* , Phys. Rev. D16 (1977) 3103.
- [12] K. L. Miller *et al* , Phys. Rev. D26 (1982) 537.
- [13] W. A. Mann *et al* , Phys. Rev. Lett. 31 (1973) 844.
- [14] N. J. Baker *et al* , Phys. Rev. D23 (1981) 2499.
- [15] T. Kitagaki *et al* , Phys. Rev. D28 (1983) 436.
- [16] T. Kitagaki *et al* , Phys. Rev. D42 (1990) 1331.
- [17] M. Holder *et al* , Nuovo Cim. ALVII (1968) 338.
- [18] R. L. Kustom *et al* , Phys. Rev. Lett. 22 (1969) 1014.
- [19] D. Perkins, in: *Proceedings of the 16th International Conference on High Energy Physics*, J. D. Jackson, A. Roberts (eds.), National Accelerator Laboratory, Batavia, Illinois, 1973, Vol. IV, 189.
- [20] A. Orkin-Lecourtois and C. A. Piketty, Nuovo Cim. AL (1967) 927.
- [21] S. Bonetti *et al* , Nuovo Cim. A38 (1977) 260.
- [22] N. Armenise *et al* , Nucl. Phys. B152 (1979) 365.
- [23] I. Budagov *et al* , Lett. Nuovo Cim. II (1969) 689.
- [24] A. Liesenfeld *et al* , Phys. Lett. B468 (1999) 20.
- [25] E. Amaldi *et al* , Nuovo Cimento A65 (1970) 377.
- [26] E. Amaldi *et al* , Phys. Lett. B41 (1972) 216.
- [27] E.D. Bloom *et al* , Phys. Rev. Lett. 30 (1973) 1186.
- [28] P. Brauel *et al* , Phys. Lett. B45 (1973) 389.
- [29] A. del Guerra *et al* , Nucl. Phys. B99 (1975) 253.
- [30] A. del Guerra *et al* , Nucl. Phys. B107 (1976) 65.
- [31] P. Joos *et al* , Phys. Lett. B62 (1976) 230.
- [32] A. S. Esaulov, A. M. Pilipenko, Yu. I. Titov, Nucl. Phys. B136 (1978) 511.
- [33] M. G. Olsson, E. T. Osypowski and E. H. Monsay, Phys. Rev. D17 (1978) 2938.

- [34] S. Choi, *Étude expérimentale et théorique de l'électroproduction de pions près du seuil et mesure des facteurs de forme axial et pseudo-scalaire*, Saclay report DAPNIA/SPhN 93 18, 1993.
- [35] D. Baumann, U. Müller *et al* (A1 Collaboration), *forthcoming*.
- [36] Y. Nambu and D. Lurié, Phys. Rev. 125 (1962) 1429.
- [37] Y. Nambu and E. Shrauner, Phys. Rev. 128 (1962) 862.
- [38] Y. Nambu and M. Yoshimura, Phys. Rev. Lett. 24 (1970) 25.
- [39] G. Furlan, N. Paver and C. Verzegnassi, Nuovo Cim. A LXX (1970) 247.
- [40] C. Verzegnassi, Springer Tracts in Modern Physics 59 (1971) 154.
- [41] G. Furlan, N. Paver and C. Verzegnassi, Springer Tracts in Modern Physics 62 (1972) 118.
- [42] N. Dombey and B. J. Read, Nucl. Phys. B60 (1973) 65.
- [43] B. J. Read, Nucl. Phys. B74 (1974) 482.
- [44] G. Benfatto, F. Nicolò and G. C. Rossi, Nucl. Phys. B50 (1972) 205.
- [45] G. Benfatto, F. Nicolò and G. C. Rossi, Nuovo Cim. A14 (1973) 425.
- [46] S. Weinberg, Phys. Rev. Lett. 4 (1960) 575.
- [47] E.J. Bleser *et al* , Phys. Rev. Lett. 8 (1962) 288.
- [48] J.E. Rothberg *et al* , Phys. Rev. 132 (1963) 2664.
- [49] E. Bertolini *et al* , Proc. Intern. Conf. on High-energy physics (CERN, Geneva 1962) p. 421;
S. Focardi *et al* , Proc. Intern. Conf. on Fundamental aspects of weak interactions (BNL, Upton, 1964), p. 278.
- [50] V.M. Bystritskii *et al* , Sov. Phys. JETP 39 (1974) 19.
- [51] G. Bardin *et al* , Nucl. Phys. A352 (1981) 365.
- [52] G. Bardin *et al* , Phys. Lett. 104B (1981) 320.
- [53] D.D. Bakalov, M.P. Faifman, L.I. Ponomarev and S.I. Vinitsky, Nucl. Phys. A384 (1982) 302.
- [54] S.-I. Ando, K. Kubodera and F. Myhrer, *in preparation*.
- [55] D.V. Balin *et al* , PSI-proposal R-97-05.
- [56] D.F. Measday, *The Nuclear Physics of Muon Capture*, Phys. Rept., in print.
- [57] Ch. Briancon *et al* , Nucl. Phys. A671 (2000) 647.
- [58] P. Ackerbauer, Phys. Lett. B417 (1998) 224.
- [59] G.H. Miller, Phys. Lett. 41B (1972) 50.
- [60] F.R. Kane, Phys. Lett. 45B (1973) 292.
- [61] P. Guichon, Phys. Rev. C19 (1979) 987.
- [62] G. Jonkmans *et al* , Phys. Rev. Lett. 77 (1996) 4512.
- [63] D.H. Wright *et al* , Phys. Rev. C57 (1998) 373.
- [64] D. Beder and H.W. Fearing, Phys. Rev. D39 (1989) 3493.
- [65] S. Choi *et al* , Phys. Rev. Lett. 71 (1993) 3927.
- [66] P. Bartsch *et al* (A1 Collaboration), MAMI-proposal A1/1-98.
- [67] C. Llewellyn Smith, Phys. Rept. 3C (1972) 261.
- [68] E. Fischbach *et al* , Phys. Rev. D15 (1977) 97.
- [69] J. Kim *et al* , Rev. Mod. Phys. 53 (1981) 211.
- [70] J. Collins, F. Wilczek and A. Zee, Phys. Rev. D18 (1978) 242.
- [71] D.B. Kaplan and A.V. Manohar, Nucl. Phys. B310 (1988) 527.
- [72] W.M. Alberico, S.M. Bilenky and C. Maieron, *subm. to Phys. Rept.*, hep-ph/0102269.
- [73] E. Amaldi, S. Fubini and G. Furlan, Springer Tracts in Modern Physics 83 (1979) 6.
- [74] V. Bernard, N. Kaiser, T.-S.H. Lee and Ulf-G. Meißner, Phys. Rept. 246 (1994) 315.
- [75] F.A. Berends, A. Donnachie and D.L. Weaver, Nucl. Phys. B4 (1967) 1.
- [76] J. Bernstein, S. Fubini, M. Gell-Mann and W. Thirring, Nuovo Cimento 17 (1960) 757.
- [77] S. Coleman, *Aspects of Symmetry* (Cambridge University Press, Cambridge, 1985).
- [78] H. Georgi, Ann. Rev. Nucl. Part. Sci. 43 (1993) 209.
- [79] Ulf-G. Meißner, Rep. Prog. Phys. 56 (1993) 903.
- [80] A. Pich, Rep. Prog. Phys. 58 (1995) 563.
- [81] G. Ecker, Prog. Part. Nucl. Phys. 35 (1995) 1.

- [82] V. Bernard, N. Kaiser and Ulf-G. Meißner, *Int. J. Mod. Phys. E4* (1995) 193.
- [83] C. Vafa and E. Witten, *Nucl. Phys. B234* (1984) 173.
- [84] S. Weinberg, *Physica* 96A (1979) 327.
- [85] J. Gasser and H. Leutwyler, *Ann. Phys.* 158 (1984) 124.
- [86] H. Leutwyler, *Ann. Phys.* 235 (1994) 165.
- [87] Ulf-G. Meißner, in: Boris Ioffe Festschrift *At the Frontier of Particle Physics - Handbook of QCD*, Vol. 1, pp. 417-501, Ed. M. Shifman (World Scientific, Singapore, 2001).
- [88] E. Jenkins and A.V. Manohar, *Phys. Lett. B255* (1991) 558.
- [89] V. Bernard, N. Kaiser and Ulf-G. Meißner, *Nucl. Phys. A615* (1997) 483.
- [90] S. Fubini, G. Furlan and C. Rosetti, *Nuovo Cim.* 40 (1965) 1171.
- [91] Riazuddin and B.W. Lee, *Phys. Rev.* 146 (1966) B1202.
- [92] S.L. Adler and F.J. Gilman, *Phys. Rev.* 152 (1966) B1460.
- [93] S.L. Adler, *Ann. Phys. (NY)* 50 (1968) 189.
- [94] G. Ecker and Ulf-G. Meißner, *Comm. Nucl. Part. Phys.* 21 (1995) 347.
- [95] V. Bernard, N. Kaiser and Ulf-G. Meißner, *Phys. Rev. Lett.* 69 (1992) 1877.
- [96] A. Schmidt, *Pion-Elektroproduktion nahe der Schwelle in chiraler Störungstheorie*, PhD thesis, TU München (1995).
- [97] K. Blomquist *et al* (A1 Collaboration), *Z. Phys.* A353 (1996) 415.
- [98] D. Drechsel, L. Tiator, *J. Phys. G: Nucl. Part. Phys.* 18 (1992) 449.
- [99] S. Amendolia *et al* (NA7 Collaboration), *Nucl. Phys. B277*, 168 (1986).
- [100] J. Bijnens, G. Colangelo and P. Talavera, *JHEP* 9805 (1998) 014.
- [101] J. Gasser and Ulf-G. Meißner, *Nucl. Phys. B357* (1991) 90.
- [102] B. Kubis and Ulf-G. Meißner, *Nucl. Phys. A671* (2000) 332.
- [103] V. Bernard, N. Kaiser, J. Kambor and Ulf-G. Meißner, *Nucl. Phys. B388* (1992) 315.
- [104] T. Becher and H. Leutwyler, *Eur. J. Phys. C9* (1999) 643.
- [105] V. Bernard, N. Kaiser and Ulf-G. Meißner, *Phys. Rev. C62* (2000) 028201.
- [106] S. Scherer and J.H. Koch, *Nucl. Phys. A534* (1991) 461 and references therein.
- [107] V. Bernard, N. Kaiser and Ulf-G. Meißner, *Phys. Rev. D50* (1994) 6899.
- [108] H.W. Fearing, R. Lewis, N. Mobed and S. Scherer, *Phys. Rev. D56* (1997) 1783.
- [109] J. Gasser, M.E. Sainio and A. Svarc, *Nucl. Phys. B307* (1988) 779.
- [110] N. Fettes, Ulf-G. Meißner and S. Steininger, *Nucl. Phys. A640* (1998) 199.
- [111] V. Bernard, N. Kaiser, J. Kambor and Ulf-G. Meißner, *Nucl. Phys. B388* (1992) 315.
- [112] S.L. Adler and Y. Dothan, *Phys. Rev.* 151 (166) 1267.
- [113] L. Wolfenstein, in: *High-Energy Physics and Nuclear Structure*, ed. S. Devons (Plenum, New York, 1970) p.661.
- [114] G. Höhler, in *Landolt-Börnstein*, vol. 9b2, ed. H. Schopper (Springer, Berlin, 1983).
- [115] R.A. Arndt, I.I. Strakovsky and R.L. Workman, *Phys. Rev. C52* (1995) 2246.
- [116] V. Bernard, T.R. Hemmert and Ulf-G. Meißner, *Nucl. Phys. A686* (2001) 290.
- [117] S.-I. Ando, F. Myhrer and K. Kubodera, *Phys. Rev. C63* (2000) 015203.
- [118] T.R. Hemmert, B.R. Holstein and J. Kambor, *J. Phys. G24* (1998) 1831.
- [119] P. Mergell, Ulf-G. Meißner and D. Drechsel, *Nucl. Phys. A597* (1995) 367.
- [120] H.-W. Hammer, Ulf-G. Meißner and D. Drechsel, *Phys. Lett. B385* (1996) 343.
- [121] V. Bernard, H.W. Fearing, T.R. Hemmert and Ulf-G. Meißner, *Nucl. Phys. A635* (1998) 121.
- [122] B. Kubis and Ulf-G. Meißner, *Nucl. Phys. A679* (2001) 698.
- [123] G.I. Opat, *Phys. Rev.* 134 (1964) B428.
- [124] H. Primakoff, *Rev. Mod. Phys.* 31 (1959) 802.
- [125] A. Santisteban and R. Pascual, *Nucl. Phys. A260* (1960) 392.
- [126] W.R. Wessel and P. Phillipson, *Phys. Rev. Lett.* 13 (1964) 23.
- [127] D. Beder, *Nucl. Phys. A258* (1976) 447.
- [128] H.W. Fearing, *Phys. Rev. C21* (1980) 1951.
- [129] D. Beder and H.W. Fearing, *Phys. Rev. D35* (1987) 2130.

- [130] T. Meissner, F. Myhrer and K. Kubodera, Phys. Lett. B416 (1998) 36.
- [131] S.-I. Ando and D.-P. Min, Phys. Lett. B417 (1998) 177.
- [132] N.C. Mukhopadhyay, in Proceedings of WEIN-98 (Santa Fe, NM, 1998), `nuc1-th/9810039`.
- [133] R. Dashen and M. Weinstein, Phys. Rev. 188 (1969) 2330.
- [134] N.H. Fuchs, H. Sazdjian and J. Stern, Phys. Lett. B238 (1990) 380.
- [135] J.L. Goity, R. Lewis, M. Schvellinger and L.-Z. Zhang, Phys. Lett. B454 (1999) 115.
- [136] B.R. Holstein, Few Body Syst. Suppl. 11 (1999) 116.
- [137] H. Leutwyler, Phys. Lett. B378 (1996) 313.
- [138] R.G.E. Timmermans, T.A. Rijken and J.J. de Swart, Phys. Lett. B257 (1991) 227; Nucl. Phys. A585 (1995) 143c.
- [139] A.D. Martin, Nucl. Phys. B179 (1981) 33.
- [140] R.A. Adelseck and B. Saghai, Phys. Rev. C42 (1990) 108.
- [141] H. Haberzettl, C. Bennhold, T. Mart and T. Feuster, Phys. Rev. C58 (1998) 40.
- [142] Ulf-G. Meißner and J.A. Oller, Nucl. Phys. A673 (2000) 311.
- [143] J.A. Oller and Ulf-G. Meißner, Phys. Lett. B500 (2001) 263.
- [144] N. Kaiser, T. Waas and W. Weise, Nucl. Phys. A612 (1997) 297.
- [145] E. Oset *et al* , Prog. Part. Nucl. Phys. 44 (2000) 213.